

**Anthropogenic,
biomass burning, and
volcanic emissions of
BC, OC, and SO₂**

T. Diehl et al.

**Anthropogenic, biomass burning, and
volcanic emissions of black carbon,
organic carbon, and SO₂ from 1980 to
2010 for hindcast model experiments**

T. Diehl^{1,2}, A. Heil³, M. Chin², X. Pan^{4,2}, D. Streets⁵, M. Schultz³, and S. Kinne⁶

¹Universities Space Research Association, Columbia, Maryland, USA

²NASA Goddard Space Flight Center, Greenbelt, Maryland, USA

³Forschungszentrum Jülich, Jülich, Germany

⁴Morgan State University, Baltimore, Maryland, USA

⁵Argonne National Laboratory, Argonne, Illinois, USA

⁶Max Planck Institute for Meteorology, Hamburg, Germany

Received: 31 July 2012 – Accepted: 27 August 2012 – Published: 21 September 2012

Correspondence to: T. Diehl (thomas.diehl@nasa.gov)

Published by Copernicus Publications on behalf of the European Geosciences Union.

Title Page

Abstract

Introduction

Conclusions

References

Tables

Figures

⏪

⏩

◀

▶

Back

Close

Full Screen / Esc

Printer-friendly Version

Interactive Discussion

Abstract

Two historical emission inventories of black carbon (BC), primary organic carbon (OC), and SO₂ emissions from land-based anthropogenic sources, ocean-going vessels, air traffic, biomass burning, and volcanoes are presented and discussed for the period 1980–2010. These gridded inventories are provided to the internationally coordinated AeroCom Phase II multi-model hindcast experiments. The horizontal resolution is 0.5° × 0.5° and 1.0° × 1.0°, while the temporal resolution varies from daily for volcanoes to monthly for biomass burning and aircraft emissions, and annual averages for land-based and ship emissions. One inventory is based on inter-annually varying activity rates of land-based anthropogenic emissions and shows strong variability within a decade, while the other one is derived from interpolation between decadal endpoints and thus exhibits linear trends within a decade. Both datasets capture the major trends of decreasing anthropogenic emissions over the USA and Western Europe since 1980, a sharp decrease around 1990 over Eastern Europe and the former USSR, and a steep increase after 2000 over East and South Asia. The inventory differences for the combined anthropogenic and biomass burning emissions in the year 2005 are 34 % for BC, 46 % for OC, and 13 % for SO₂. They vary strongly depending on species, year and region, from about 10 % to 40 % in most cases, but in some cases the inventories differ by 100 % or more. Differences in emissions from wild-land fires are caused only by different choices of the emission factors for years after 1996 which vary by a factor of about 1 to 2 for OC depending on region, and by a combination of emission factors and the amount of dry mass burned for years up to 1996. Volcanic SO₂ emissions, which are only provided in one inventory, include emissions from explosive, effusive, and quiescent degassing events for 1167 volcanoes.

Anthropogenic, biomass burning, and volcanic emissions of BC, OC, and SO₂

T. Diehl et al.

Title Page

Abstract

Introduction

Conclusions

References

Tables

Figures



Back

Close

Full Screen / Esc

Printer-friendly Version

Interactive Discussion



1 Introduction

The atmospheric aerosol has the highest uncertainty among the components contributing to anthropogenic climate forcing, as summarized in the Fourth Assessment Report of the Intergovernmental Panel on Climate Change (IPCC AR4, Forster et al., 2007) and in the 2009 US Climate Change Science Program report (CCSP, 2009). This uncertainty is largely due to insufficient knowledge of the aerosol physical, chemical, and optical properties, emissions of aerosols and their precursors, removal processes, and aerosol-cloud interactions. Aerosols affect the climate and weather by absorbing or scattering solar radiation, and by changing cloud formation, precipitation, and the atmospheric dynamics. Aerosols also impact air quality and visibility, and cause concerns for human health.

Aerosols are composed of different species, mainly dust, sea salt, sulfate, black carbon (BC), organic carbon (OC), among others, originating from a variety of sources including fossil fuel and biofuel combustion, biomass burning from wildfires and agriculture practice, deserts, oceans, terrestrial and oceanic biogenic sources, and volcanoes. The amount of aerosols injected into the atmosphere by human activities has increased substantially since the pre-industrial era. In the last 30 yr, anthropogenic sources have changed significantly in different regions of the world due to various economic and policy factors, decreasing in some regions (e.g. North America and Europe) and rising in other regions (e.g. China and India). These emission changes have been linked to observed variations of the Aerosol Optical Depth (AOD) (Streets et al., 2009). It is important to understand the quantitative relationship between emission changes and changes of the atmospheric loading and radiative forcing in the past in order to make assessments of future climate changes with projected emission scenarios. Another important aspect is to evaluate the impact of emission changes in one region on the air quality in other regions via long-range transport of aerosols.

We present here a compilation of anthropogenic, biomass burning, and volcanic emissions of BC, OC, and SO₂ (a precursor gas of sulfate aerosols) in the past three

ACPD

12, 24895–24954, 2012

Anthropogenic, biomass burning, and volcanic emissions of BC, OC, and SO₂

T. Diehl et al.

Title Page

Abstract

Introduction

Conclusions

References

Tables

Figures



Back

Close

Full Screen / Esc

Printer-friendly Version

Interactive Discussion

Anthropogenic, biomass burning, and volcanic emissions of BC, OC, and SO₂

T. Diehl et al.

Title Page

Abstract

Introduction

Conclusions

References

Tables

Figures

⏪

⏩

◀

▶

Back

Close

Full Screen / Esc

Printer-friendly Version

Interactive Discussion



decades for global model hindcast studies, as part of a project supported by NASA's Modeling, Analysis and Prediction (MAP) program. This emission inventory contains inter-annually varying anthropogenic and seasonally varying biomass burning emissions from 1980 to 2007, and the continuously degassing and eruptive volcanic emissions from 1980 to 2009. This period is chosen because not only is it characterized by considerable changes of regional emissions, but also by the availability of global aerosol observations from several satellite instruments, e.g. the Advanced Very High Resolution Radiometer (AVHRR) since 1981, the Total Ozone Mapping Spectrometer (TOMS) from 1979 to 2001, and the Moderate Resolution Imaging Spectroradiometer (MODIS) and the Multi-angle Imaging SpectroRadiometer (MISR) instruments since 2000.

Thus, the purpose of aerosol hindcast studies is to evaluate the skill of models to reproduce observed trends of concentrations, total aerosol optical depth and radiative fluxes (for both clear-sky and all-sky), and to assess the relative impact of anthropogenic emission trends versus climate trends and/or climate variability on these quantities. A major aerosol model hindcast activity has been organized and coordinated by the international Aerosol Comparisons between Observations and Models (AeroCom) project, which was initiated in 2002 with the overall goal to reduce the uncertainty of the aerosol impact on the climate system (Schulz et al., 2009; <http://aerocom.met.no>). To facilitate this task, AeroCom coordinates model experiments and their analysis among aerosol groups in order to determine the model diversity of estimated anthropogenic aerosol climate forcing and associated atmospheric processes. Currently, more than 15 models are participating in AeroCom. In the first phase of model experiments (AeroCom Phase I), a series of model experiments (A, B and PRE) were conducted and results have been presented in several publications (Textor et al., 2006, 2007; Kinne et al., 2006; Schulz et al., 2006; Penner et al., 2006; Koch et al., 2009; Huneus et al., 2011; Koffi et al., 2012). AeroCom results have contributed to the IPCC AR4 on aerosol climate forcing assessment.

Anthropogenic, biomass burning, and volcanic emissions of BC, OC, and SO₂

T. Diehl et al.

Title Page

Abstract

Introduction

Conclusions

References

Tables

Figures



Back

Close

Full Screen / Esc

Printer-friendly Version

Interactive Discussion



Despite some improvement of our knowledge of aerosol sources and properties, there is still significant uncertainty in many processes and consequently in assessing the anthropogenic aerosol climate forcing. To address these open questions, a second phase of AeroCom multi-model experiments (AeroCom Phase II) has been designed.

5 One of these experiments, the hindcast experiment, was designed in collaboration with the Atmospheric Chemistry and Climate Initiative (AC&C), a joint project of the International Global Atmospheric Chemistry (IGAC) project and the Stratospheric Processes And their Role in Climate (SPARC) project. AC&C has established several collaborative projects, including a hindcast study for both aerosols and trace gases (AC&C1) and a time-slice study (formerly called AC&C4), known as Atmospheric Chemistry and Climate Model Intercomparison Project (ACCMIP) (Shindell et al., 2009). It is anticipated that results from the AeroCom Phase II and AC&C studies will inform the IPCC for its 5th Assessment Report (AR5).

To facilitate hindcast experiments undertaken by AeroCom, the multi-decadal emission inventories created in the MAP project and ACCMIP were made available to the AeroCom modeling community. In addition, AeroCom also archives emissions datasets representative of the pre-industrial era for 1750 (Dentener et al., 2006) and 1850 (Lamarque et al., 2010), which can be used for aerosol direct forcing experiments.

20 This paper describes two global emission inventories used in the AeroCom Phase II hindcast model experiments. The first one is the MAP inventory, referred to as A2-MAP in this paper, The second one contains historic emissions which Lamarque et al. (2010) created for the ACCMIP project from 1850 to 2000 in decadal increments, and projected emissions for 2005 and 2010 from the Representative Concentration Pathways (RCP) 8.5 scenario (Riahi et al., 2011). This dataset, referred to as A2-ACCMIP in this paper, covers the period 1980 to 2010. It is also described in Granier et al. (2011) (referred to as MACCity).

25 In the remainder of this paper, we will discuss the methodologies used to create the A2-MAP and A2-ACCMIP inventories, analyze their temporal and spatial features, and discuss the application of the two datasets.

2 Methodology for the A2-MAP emissions

2.1 Land-based anthropogenic emissions

We compiled a gridded inventory in a resolution of $1.0^\circ \times 1.0^\circ$ of land-based anthropogenic emissions of black carbon (BC), primary organic carbon (OC), and SO_2 (as a precursor of sulfate) as annual emissions from 1980–2007.

For BC and OC, the basis for this inventory is a gridded inventory for the year 1996 from Bond et al. (2004) and yearly global emission trends for 17 regions from Streets et al. (2006, 2008, 2009). For each year y and region r , a regional scaling factor $F_{r,y}$ was calculated as

$$F_{r,y} = \frac{\sum_{i=1, n_r} E_{i,y}}{\sum_{i=1, n_r} E_{i,1996}} \quad (1)$$

where the sum extends over all n_r grid points in a given region, and $E_{i,y}$ are the emissions in a grid box for the specified year. These scaling factors were then applied to all grid points within this region to generate the gridded emissions for the individual years. The 17 regions are shown in Fig. 1 (same as used in the IMAGE 2.2 model, see IMAGE team, 2001, and Eickhout et al., 2004). A global gridded bitmap of these regions was derived by assigning region numbers to individual countries in a country map.

Bond et al. (2004) used a technology-based approach to calculate emissions per country, by combining data on fuel usage and type, emission factors, combustion technologies and practices, and particle filtering devices. The emissions are then approximated by summing over all combinations of sector, fuel, and technology. Fuel data is mostly from the International Energy Agency (IEA, 1998a, b), while the emission factors are based on an extensive literature review. The methodology was implemented in the software package “Speciated Pollutant Emissions Wizard” (SPEW). In order to

Anthropogenic, biomass burning, and volcanic emissions of BC, OC, and SO_2

T. Diehl et al.

Title Page

Abstract

Introduction

Conclusions

References

Tables

Figures

⏪

⏩

◀

▶

Back

Close

Full Screen / Esc

Printer-friendly Version

Interactive Discussion

map the emissions onto a grid, the authors used mainly the proxies total population, and fraction of urban and rural population.

Streets et al. (2006, 2008, 2009) have further extended the BC and OC emissions to cover the period of 1980 to 2006, using annual fuel-use data from the IMAGE model version 2.2 (Eickhout et al., 2004; IMAGE team, 2001) for a number of world regions and economic sectors, as well as official Chinese energy statistics. It also accounts for changes in technology and emission control measures over this period, and uses 112 fuel/sector/technology combinations. These regional emissions are mapped to the $1^\circ \times 1^\circ$ grid based on the spatial distribution from the 1996 BC and OC emission map described above, assuming no changes in the spatial pattern during the 27-yr period.

For SO_2 , a first version of A2-MAP (A2-MAP-v1) was generated based on a gridded map for the year 2000 from the EDGAR 3.2 Fast Track 2000 dataset (EDGAR 32FT2000, Olivier et al., 2005), and yearly regional trends developed by Streets et al. (2006, 2008, 2009). These annual trends of SO_2 were estimated by adapting the approach for the BC and OC trends to the case of SO_2 emissions, taking into account trends for fuel sulfur content, and flue gas desulfurization. We performed the mapping of the regional trends as in Eq. (1), with 1996 replaced by 2000. However, the SO_2 trend in A2-MAP-v1 over Europe is most likely overestimated after 1990 as compared to other inventories (Granier et al., 2011), and it is the only inventory that shows an increasing trend over Eastern Europe, which is inconsistent with major economic changes in this timeframe (Vestreng et al., 2007). In order to correct this issue, we replaced the SO_2 emissions in a second version (A2-MAP-v2) with SO_2 emissions from the EDGAR 4.1 inventory (European Commission, 2010). An artifact in EDGAR 4.1 over the Indian Ocean from mislabeling a longitudinal coordinate was corrected (emission at 71.3°W , 35.8°S from a Chile copper mine was mislabeled as 71°E , 35.8°S). EDGAR 4.1 provides emissions on a $0.5^\circ \times 0.5^\circ$ grid for the years 1975, 1980, 1985, 1990, 1995, and annually from 2000–2005. We generated the remaining years before 2000 by linear interpolation. Compared to EDGAR 32FT2000, EDGAR 4.1 uses updated maps on

**Anthropogenic,
biomass burning, and
volcanic emissions of
BC, OC, and SO_2**

T. Diehl et al.

Title Page

Abstract

Introduction

Conclusions

References

Tables

Figures



Back

Close

Full Screen / Esc

Printer-friendly Version

Interactive Discussion



power plants, road transport, international shipping routes, oil refineries, and population proxies.

The major land-based anthropogenic sectors included in the A2-MAP inventory are residential (including biofuel and agricultural waste burning), industry (including biofuel), power generation (including biofuel and municipal waste burning), and transport. Emissions from ocean-going ships, air traffic, and open biomass burning are provided separately (see below). However, inland water transport is included as part of the land-based emissions.

2.2 Emissions from international ship traffic

SO₂ emissions from ocean-going ships in A2-MAP-v1 were derived from the gridded SO₂ emission dataset labeled “SHIP-EYRING” (Eyring et al., 2005a) for the year 2000 in a resolution of 1° × 1°, distributed as part of EDGAR 32FT2000. Eyring et al. (2005a) combine information on engine types, installed engine power, average engine load, annual engine running hours, and the power-dependent fuel consumption rates and emission factors to estimate global total fuel consumption and emission of SO₂, PM₁₀, and other species, using data from Lloyd’s Maritime Information System (LMIS) (2002), and data provided by engine manufacturers. They compute the fraction of PM₁₀ attributed to BC, OC, and SO₄ based on the work of Sinha et al. (2003), and Petzold et al. (2004) as 3 %, 8 %, and 47 %, respectively (the rest is ash and other particulate matter). The total emissions of SO₂ and PM₁₀ (particulate matter with diameters less than 10 μm) for 2000 were mapped to a 1° × 1° grid by using vessel traffic densities from the Automated Mutual-assistance Vessel Rescue (AMVER) system, while emissions for 1970, 1980, 1995, and 2001 were given as the annual total amount (Eyring et al., 2005a). A projection for 2020 was published in Eyring et al. (2005b). We calculated annual ship emissions from 1980 to 2007 via linear interpolation between the available years and mapped them into the 2000 grid, assuming no change on shipping routes and PM₁₀ attributions to the individual species.

Anthropogenic, biomass burning, and volcanic emissions of BC, OC, and SO₂

T. Diehl et al.

Title Page

Abstract

Introduction

Conclusions

References

Tables

Figures

⏪

⏩

◀

▶

Back

Close

Full Screen / Esc

Printer-friendly Version

Interactive Discussion



In the second version A2-MAP-v2, we replaced the “SHIP-EYRING” map with the gridded SO₂ ship emissions available in EDGAR 4.1 with a resolution of 0.5° × 0.5°, since this inventory contained updated datasets and additional years. Similar to the land-based emissions, we used annual emissions for 1975, 1980, 1985, 1990, 1995, and 2000–2005, and interpolated the remaining years. Because EDGAR 4.1 does not provide ship emissions for BC, OC and SO₄, we kept the same emission amount of these species as in A2-MAP-v1 but gridded them onto the ship traffic patterns from EDGAR 4.1.

2.3 Aircraft emissions

The inventory of 3-dimensional gridded burned fuel for 1980–2010 provided as part of A2-MAP is based on work from Baughcum et al. (1996a, b), Sutkus et al. (2001), and Mortlock et al. (1998), published within the framework of NASA’s Atmospheric Effects of Aviation Project (AEAP) and Ultra Efficient Engine Technology (UEET) Program. These AEAP and UEET datasets include data from both scheduled air traffic as well as military and charter traffic and general aviation. The basic methodology of AEAP/UEET was a bottom-up approach, using a combination of aircraft schedules, data on combinations of aircraft types and engines, and detailed calculations of fuel burned along each flight path.

Baughcum et al. (1996a, b) and Sutkus et al. (2001) generated inventories of burned fuel for scheduled air traffic for the years 1976, 1984, 1992, and 1999. They used flight information from the Official Airline Guide (OAG), taking into account occasional duplicate listings, and added information on engine types for several airplanes included in fleet information databases available from Boeing (“Jet Track”) and the Airclaims Company. Some aircraft/engine combinations were approximated by other combinations, if not enough details on their performance characteristic were available. Aircraft performance files were generated for all the aircraft/engine combinations using the Boeing Mission Analysis Program (BMAP), providing fuel mileage as a function of weight, speed, and altitude for both taxi, climb, descent, and cruise conditions. A 70% load

**Anthropogenic,
biomass burning, and
volcanic emissions of
BC, OC, and SO₂**

T. Diehl et al.

Title Page

Abstract

Introduction

Conclusions

References

Tables

Figures



Back

Close

Full Screen / Esc

Printer-friendly Version

Interactive Discussion



factor was assumed for passenger airplanes, while payloads for freighter airplanes were derived from data reported by the US Department of Transportation (DOT). Finally, the authors used the Global Atmospheric Emissions Code (GAEC) to calculate the actual fuel burned on a sparse grid with a horizontal resolution of $1^\circ \times 1^\circ$ degrees and 25 pressure altitude levels from 0 km to 25 km, where the altitude is geopotential height and corresponds to pressures using the 1976 US Standard Atmosphere (1976). This approach was used to generate inventories of burned fuel for 1976 and 1984 (Baughcum et al., 1996a), 1992 (Baughcum et al., 1996b), and 1999 (Sutkus et al., 2001), where 1976 and 1984 are only available for February, May, August and November, while the datasets for 1992 and 1999 contain all months. Another difference is that the inventory for 1999 contains data on domestic flights within the Commonwealth of Independent States (CIS) and China, while these flights are not included in the previous years.

An emission scenario for scheduled air traffic in 2015 (without domestic traffic in CIS and China) was developed by Baughcum et al. (1998), predicting fleet mix, aircraft performance features, flight schedule changes, and demand growth for 2015. The seasonal variation was assumed to be the same as for 1992.

Yearly emission inventories for the military, charter, unreported domestic traffic (referring to CIS and China) and general aviation sectors were compiled by Mortlock et al. (1998) for 1976, 1984, 1992, and 2015. For each of these sectors, the authors specified a number of generic aircraft and engine types to determine performance capability and to model fuel burn. The authors also defined a set of route flight profiles, including flight frequency. Air traffic network models were used to generate the flight profiles for charter and unreported domestic traffic. For the military and general aviation components, aircraft were based at the center of regional areas throughout the world, and data from the US Air Force and the International Civil Aviation Organization (ICAO) were used to determine flight utilization. For the 2015 scenario, the authors consulted trend analyses from a number of sources, e.g. the Federal Aviation Authority (FAA), the

**Anthropogenic,
biomass burning, and
volcanic emissions of
BC, OC, and SO₂**T. Diehl et al.

[Title Page](#)[Abstract](#)[Introduction](#)[Conclusions](#)[References](#)[Tables](#)[Figures](#)[Back](#)[Close](#)[Full Screen / Esc](#)[Printer-friendly Version](#)[Interactive Discussion](#)

General Aviation Manufacturers Association (GAMA), and the International Institute for Strategic Studies.

The data from Mortlock et al. (1998) was used to generate a gridded dataset of burned fuel from military, charter and general aviation traffic for 1999 by applying annual growth rates from the global fuel use for the respective components between 1992 and 2015. Total gridded aircraft fuel usage for 1999 was then derived by summing these components and the scheduled traffic data for 1999. For all other years (1976, 1984, 1992, 2015), the data from Mortlock et al. (1998) and the data from scheduled traffic was also combined to yield total fuel burned (S. Baughcum, personal communication).

For all years provided in the AEAP/UEET inventory, we calculated the total amount of fuel burned and then interpolated the total fuel to the remaining years of the period 1976–2010. The gridded data for these remaining years was then generated by scaling all grid points in the original AEAP/UEET files with the total amount of fuel burned for this particular year.

2.4 Biomass burning emissions

The amount of dry mass burned in open biomass burning provided within A2-MAP is based on the GFED-v2 inventory (Van der Werf et al., 2006; Randerson et al., 2007) for 1997 to 2007 and work from Duncan et al. (2003) for 1980 to 1996. Here, open biomass burning refers to grassland, savannah and forest fires caused by anthropogenic activities or natural events. Agricultural waste burning is included in the land-based anthropogenic emissions but not in the GFED-v2 inventory. However, it is part of the Duncan-based inventory, potentially causing a slight emission overestimate of agricultural waste burning for the period prior to 1997.

GFED-v2 provides global monthly emissions from 1997 to 2007 on a $1^\circ \times 1^\circ$ grid. Emissions of carbon are computed as

$$E_C = A \times FL \times CC \quad (2)$$

Anthropogenic, biomass burning, and volcanic emissions of BC, OC, and SO₂

T. Diehl et al.

Title Page

Abstract

Introduction

Conclusions

References

Tables

Figures

⏪

⏩

◀

▶

Back

Close

Full Screen / Esc

Printer-friendly Version

Interactive Discussion



where A is the burned area, FL the fuel load, and CC the combustion completeness. Emitted trace species are then computed as $E = DM \times EF$, where EF is the emission factor for individual species and DM the dry matter, with $DM = E_C/0.45$. The burned area was estimated for 14 regions from MODIS fire counts for 2001 to 2007, a combination of fire counts from the VIRS instrument on the TRMM satellite and the ATSR instrument on the ERS satellite for 1997–2000, as well as vegetation maps and fire persistence. The fuel load was calculated with the CASA biogeochemical model, using the NPP (derived from AVHRR's NDVI product) and other input parameters. It takes into account the combustion of organic soils and peat. CASA also computes CC , taking into account fuel type and moisture content.

Duncan et al. (2003) used an inventory of dry matter burned from Logan and Yevich as described in Lobert et al. (1999) as their starting point. This inventory was constructed with data from the 1980's. They used fire counts from AVHRR (for 1992–1994) and from ATSR (for 1996–2000) as a proxy to estimate the seasonal variability. Additionally, they used the Aerosol Index (AI) available from the TOMS instrument to determine the interannual variability from 1979 to 1999, where they filled the gap in TOMS data from May 1993 to July 1996 with data from other sources.

For the period of 1997 to 1999 where the Duncan and GFED datasets overlap, we determined a 3-yr average of scaling factors for each month and each of the 8 regions

defined in Duncan et al. (2003) as $\frac{DM_{region}^{GFED}}{DM_{region}^{Duncan}}$. These scaling factors are then applied to the whole Duncan dataset to generate a scaled version for the period 1979 to 1996. We applied this procedure because the GFED-v2 inventory is one of the most state-of-the-art biomass burning datasets that includes data from satellites on burned area and seasonality.

In A2-MAP, only DM is provided but not the actual species emissions, so that modelers have to apply their own choice of emission factors for BC , OC , and SO_2 to obtain the corresponding biomass burning emissions of each species. Discussions regarding the emission factors are given in Sect. 5.2.

**Anthropogenic,
biomass burning, and
volcanic emissions of
BC, OC, and SO₂**

T. Diehl et al.

Title Page

Abstract

Introduction

Conclusions

References

Tables

Figures



Back

Close

Full Screen / Esc

Printer-friendly Version

Interactive Discussion



2.5 Volcanic SO₂ emissions

SO₂ emissions from volcanoes are only briefly described here for the sake of completeness, and are covered in detail in a separate paper (Diehl et al., 2012).

We have compiled a database of SO₂ emissions and plume heights for 1167 volcanoes considered to be active (i.e. those with historic subaerial eruptions) in the Smithsonian Institution's Global Volcanism Program database (GVP) (Simkin and Siebert, 2002), for each day from 1 January 1979 to 31 December 2009. Emissions due to both explosive and effusive eruptions as well as due to quiescent degassing are taken into account.

The GVP database contains dates and the Volcanic Explosivity Index (VEI) for eruptive episodes, where the VEI is based on the amount of tephra ejected and/or the plume height (Newhall and Self, 1982). For each VEI, the Volcanic Sulfur Index (VSI) assigns a range of SO₂ emissions, derived from SO₂ observations of the TOMS instrument from 1979–1993 (Schnetzler et al., 1997). In our inventory, the default SO₂ approximation assigned to an eruption is based on the VSI. This data is replaced with specific observations from the TOMS and OMI satellite instruments when available, or in some cases with Correlation Spectrometer (COSPEC) measurements and more detailed analyses from the open literature. For some eruptions, the ejected lava and/or tephra volumes are known, and the SO₂ was estimated from an empirical formula of Blake (2003). Emissions from 49 quasi-continuously erupting volcanoes are from Andres and Kasgnoc (1998), while silent degassing estimates for non-eruptive periods are based on Berresheim and Jaeschke (1983), and Stoiber et al. (1987).

In our inventory, the plume height default is based on the VEI-height relationship. More detailed data from the weekly or monthly reports from GVP has been added over time. Plume heights for major eruptions are from analyses in the literature. Silently degassing volcanoes emit at the elevation of the volcano. No flank degassing is considered.

Anthropogenic, biomass burning, and volcanic emissions of BC, OC, and SO₂

T. Diehl et al.

Title Page

Abstract

Introduction

Conclusions

References

Tables

Figures



Back

Close

Full Screen / Esc

Printer-friendly Version

Interactive Discussion



3 Methodology for the A2-ACCMIP emissions

The A2-ACCMIP emission dataset has been prepared from the ACCMIP historical emission dataset described in Lamarque et al. (2010) and the so-called RCP8.5 (Representative Concentration Pathways) future emission scenario described in Riahi et al. (2011).

The ACCMIP dataset provides $0.5^\circ \times 0.5^\circ$ horizontally gridded emission estimates for 10 anthropogenic sectors and 2 biomass burning categories for the years 1850 to 2000 as monthly means in the decadal intervals, with a seasonality given only for the biomass burning data. The dataset represents a best guess emission estimate constructed from a harmonized combination of existing regional and global inventories. RCP emission estimates for the decades 2000 to 2100 (with an additional estimate for 2005) were developed as projections starting from the decade 2000 ACCMIP emissions.

The A2-ACCMIP emissions for given years (i.e. years 1850, 1980 to 2010) were calculated from linear time interpolation of ACCMIP and RCP85 data (ftp://ftp-ipcc.fz-juelich.de/pub/emissions/gridded_netcdf/) with the exception of biomass burning emissions of the years 1980 to 2008. The latter are taken from the so-called ACCMIP-MACCity biomass burning emission dataset which contains monthly mean emissions with explicit interannual variability and which is the original data used to construct the decadal mean ACCMIP biomass burning emissions (Granier et al., 2011). On a yearly average, the anthropogenic emissions of the years 1980 to 2010 contained in the A2-ACCMIP dataset are practically identical with the ACCMIP-MACCity anthropogenic emissions described in Granier et al. (2011) which contain an additional seasonality.

The ACCMIP-MACCity biomass burning emission dataset for the years 1997 to 2008 has been prepared from the GFEDv2 inventory (Global Fire Emissions Database, Version 2), described in van der Werf et al. (2006), while the years 1980 to 1996 have been prepared from the RETRO wildland fire emission inventory (version 2), described in Schultz et al. (2007, 2008). Both inventories provide monthly mean gridded global

Anthropogenic, biomass burning, and volcanic emissions of BC, OC, and SO₂

T. Diehl et al.

Title Page

Abstract

Introduction

Conclusions

References

Tables

Figures



Back

Close

Full Screen / Esc

Printer-friendly Version

Interactive Discussion



**Anthropogenic,
biomass burning, and
volcanic emissions of
BC, OC, and SO₂**T. Diehl et al.

[Title Page](#)[Abstract](#)[Introduction](#)[Conclusions](#)[References](#)[Tables](#)[Figures](#)[⏪](#)[⏩](#)[◀](#)[▶](#)[Back](#)[Close](#)[Full Screen / Esc](#)[Printer-friendly Version](#)[Interactive Discussion](#)

data on the amount of biomass burned by forest (tropical and extra-tropical) and savannah fires and derived emission estimates. The ACCMIP-MACCity biomass burning emissions were calculated from the monthly biomass burned estimates by applying fuel-type specific emission factors from Andreae and Merlet (2001, with updates until 2008), a biomass carbon content of 45 % and the GFEDv2 predominant vegetation cover map. Emissions from burning of peat soils are also explicitly taking into account. The parameterization is described in Lamarque et al. (2010). Information on the fractional distribution of peat soils is taken from the FAO (2003) WRB Map of World Soil Resources. Peat-fire specific emission factors published by Christian et al. (2003) are applied, which, for species such as CO, NH₃, CH₄ and SO₂ yield distinctively higher emissions per unit mass biomass burned than forest or savannah fires. On the other hand, the peat-fire emission factors for, e.g. BC, OC and NO_x are lower. The inclusion of peat fires may thus lead to significant regional differences in the estimated emission when compared to the original GFEDv2 or RETROv2 inventory.

For the compilation of the ACCMIP-MACCity biomass burning emissions inventory, the original spatiotemporal patterns of biomass carbon burned in the RETRO inventory have been improved (redistributed) in the RETRO regions contiguous USA, C-America, S-America, NH Africa, SH Africa, India, continental Southeast Asia and Australia. A monthly fire climatology derived from the GFEDv2 data (mean over years 1997 to 2006) was used to redistribute in space and time the regional annual total carbon emissions of each of these regions. For the RETRO region Siberia and Mongolia, the redistribution was done using combined information from the GFEDv2 monthly climatology and monthly Fire Danger Index (FDI) maps for the period. The original spatiotemporal carbon emission patterns of Alaska, Canada, Europe and Indonesia remained unchanged.

Given the above-described approach, the A2-ACCMIP biomass burning emission dataset has two discontinuities: one between 1996 and 1997 and another one between 2008 and 2009. This is because the spatiotemporal pattern of fire emissions in the period 1997 to 2008 is derived from satellite observations of actual fires (GFEDv2

inventory) while the patterns before 1997 (modified RETRO inventory) and after 2008 (linear time interpolation of the RCP8.5 inventory) are derived from fire climatologies.

4 Results

4.1 Land-based anthropogenic emissions

5 For the discussion of land-based anthropogenic emissions, we first focus on the trends in the following six IMAGE 2.2 regions as defined in Fig. 1: USA, OECD Europe, Eastern Europe, Former USSR, South Asia, and East Asia. These regions are chosen because they exhibit significant emission changes over the last 30 yr, particularly for SO₂. For A2-MAP-v2, the fraction of global land-based anthropogenic emissions attributed to these 6 regions in 2005 is 62 % for BC, 57 % for OC, and 65 % for SO₂ (Table 1). It should be pointed out that there is generally more temporal variation within the A2-MAP-v1 inventory than in A2-ACCMIP, since this inventory is based on actual reported annual data (like activity rates), while A2-ACCMIP is interpolated from decadal ACCMIP values and therefore has no fluctuations within a decade by construction. A2-MAP-v2 is somewhere in between, with reported data for every 5 yr up to 2000, and subsequent annual data. This different feature becomes even more pronounced on a regional basis. Whether this additional temporal information is important depends on the specific application the inventories are used for.

4.1.1 Regional SO₂ emissions

20 All 3 inventories show an overall reduction of SO₂ emissions for the USA in Fig. 2, although the A2-MAP-v2 emissions are higher in the 1980s. The overall decrease seen in all inventories can be attributed to environmental legislation and specifically to implementation of flue-gas desulfurization (FGD) units (also known as “scrubbers”) in power plants (see, e.g. the US national emissions inventory: <http://www.epa.gov/ttn/chief/eiinformation.html>). For OECD Europe the emissions decrease in all inventories

Anthropogenic, biomass burning, and volcanic emissions of BC, OC, and SO₂

T. Diehl et al.

Title Page

Abstract

Introduction

Conclusions

References

Tables

Figures



Back

Close

Full Screen / Esc

Printer-friendly Version

Interactive Discussion



Anthropogenic, biomass burning, and volcanic emissions of BC, OC, and SO₂

T. Diehl et al.

Title Page

Abstract

Introduction

Conclusions

References

Tables

Figures

⏪

⏩

◀

▶

Back

Close

Full Screen / Esc

Printer-friendly Version

Interactive Discussion

up to about 2000, after which the A2-MAP-v1 data is leveling off. The decrease is due to the same reasons as for the USA. The A2-MAP-v1 emissions after 2000 might be overestimated, although to a smaller degree as in the Eastern European case. In Eastern Europe, A2-ACCMIP and A2-MAP-v2 emission trends are similar, although the difference is 50 % in 2005, possibly due to scenario data used in A2-ACCMIP for this year. The A2-MAP-v1 emissions exhibit a significantly different pattern, with an increase in the late 1980s and another increase from 1994 on. As pointed out in Granier et al. (2011), the decrease of emissions in Eastern Europe as a result of the breakdown of communism and subsequent regulatory efforts is well documented. SO₂ reduction measures were apparently not taken fully into account within this region (and possibly also within OECD Europe after 2000) in the construction of A2-MAP-v1, which was the reason why we replaced it with the A2-MAP-v2 dataset.

In the former USSR, the inventories show discrepancies up to 82 % during the 1980s, but agree on a steep decline in the early 1990s, consistent with the breakdown of communism and the economy in this period. From 1995 on, the A2-ACCMIP emissions continue to decrease, while the other inventories level off or show even a slight increase.

In South Asia, all inventories agree on a continuous upward trend, with differences from about 40 % in 1980 to less than 10 % in 2005. This growth is mainly caused by increasing activities in the emergent Indian economy. As a result of the booming economy in China, the East Asian emissions increase as well throughout most of the time frame 1980–2005, with a particular steep increase between 2000 and 2005 (over 50 %). The one exception to this trend is a decrease between 1995 and 2000, which has been attributed to the Asian economic crisis, a decline in coal use in the residential and industrial sectors, and a reduction of the sulfur content of coal in China (Streets et al., 2003; Ohara et al., 2007). This decline is not included in A2-ACCMIP since it was derived from ACCMIP which has a coarser temporal resolution. The reduction of emissions after 2006 shown by A2-ACCMIP was also reported by Lu et al. (2011), although their emissions remain at a higher level (31 Tg (China) in Lu et al. (2011)

vs 28 Tg (East Asia) in A2-ACCMIP for 2010). Lu et al. (2011) used updated and more detailed information about activity rates and other data for both China and India to generate gridded emissions of BC, OC, and SO₂ from 1996–2010 with monthly variability. A2-MAP-v1 has the highest emissions throughout the whole period (up to 50 % higher than A2-ACCMIP), while the values from A2-MAP-v2 lie in between.

The general downward and upward emission trends over USA/Europe and China/India, respectively, are also consistent with studies analyzing aerosol optical depth (AOD) trends from SeaWiFS for the timeframe 1997–2008 (2010) from Yoon et al. (2011) and Hsu et al. (2012), at least for the pollution dominated seasons.

4.1.2 Regional BC emissions

Generally, BC emissions for the USA have been reduced since 1980 in both inventories shown in Fig. 3, but there is a slight increase since 2000 in A2-MAP-v1, while A2-ACCMIP shows a decline in this period. The step function visible in the USA emissions is actually present in the reported fuel use data. For example, between 1995 and 1996 there was a decline in residential solid fuel use and in some transportation sectors (not shown). For OECD Europe, the overall decrease of emissions from 1980 to 2005 depicted by both inventories is about 16 %. Both show opposite trends after 2000, as for the USA. In Eastern Europe, a decline occurs around 1990, consistent with political and economic changes. However, the downward trend in A2-ACCMIP ends in 1990 as a result of the interpolation, while in A2-MAP-v2 it continues to 1992, with a decline of 47 %. For subsequent years, the two inventories have rather flat emissions, again with slightly opposite trends after 2000. Similarly, both inventories show a decline in the former USSR around 1990, but the decline is more pronounced than for Eastern Europe (about 66 % for A2-MAP-v1 from 1985 to 1995). The emissions in the two inventories are practically identical in some years and have a maximum difference of about 100 %. The opposing trend pattern after 2000 is present over this region as well.

As for SO₂, the inventories show continuously increasing emissions over South Asia, increasing by 45 % over the period. Emissions in the two inventories agree within a few

**Anthropogenic,
biomass burning, and
volcanic emissions of
BC, OC, and SO₂**

T. Diehl et al.

Title Page

Abstract

Introduction

Conclusions

References

Tables

Figures



Back

Close

Full Screen / Esc

Printer-friendly Version

Interactive Discussion



percent for some years and show a maximum deviation of about 25 %. There is agreement over East Asia on an overall growth of 60 % from 1980 to 2005, and a steep increase after 2000 (20 % within 5 yr). The agreement lies again within a few percent for some years, while the maximum emission difference is about 15 %. A2-MAP-v1 shows a short decline between 1995 and 2000. Like A2-ACCMIP, Lu et al. (2011) also report a further increase after 2006.

4.1.3 Regional OC emissions

OC emissions over the USA agree within 17 % (Fig. 4), with a decline in the 1980s, and again slightly opposite trends after 2000. Emissions decrease by about 30 % in both inventories over OECD Europe, and the same slightly opposite trend patterns occur after 2000. Both inventories display similar downward trends in Eastern Europe, with differences varying between 10 % and 30 % . Emissions decline around 1990, and stay approximately flat for subsequent years up to 2005, with no opposing trends after 2000 in this case.

There is less agreement in case of the former USSR, where A2-ACCMIP is larger by a factor of 2 to more than 5. Both datasets show a decline until the mid-1990s, after which A2-MAP-v1 stays flat, while A2-ACCMIP continues to decrease. Both inventories exhibit a continuous increase over South Asia, although the increase is lower in A2-MAP-v1 after the mid-1990s. A2-ACCMIP emission are higher by approximately 25 % for most years. Finally, emissions over East Asia are also higher in A2-ACCMIP than in A2-MAP-v1, from about 30 % up to 60 %. There is an increasing trend present in both inventories, with an overall growth of 30 %–40 %. A2-MAP-v1 again shows a short decline between 1995 and 2000. Like A2-ACCMIP, Lu et al. (2011) also report a further increase after 2006. Deviating from the steep increase between 2000 and 2005 for BC and SO₂, A2-ACCMIP slightly decreases within this time frame.

Although the general OC trend patterns for the former USSR, South Asia, and East Asia are similar to the BC trends and also similar among the inventories, the relative differences between A2-ACCMIP and A2-MAP-v1 are larger for OC than for BC in these

**Anthropogenic,
biomass burning, and
volcanic emissions of
BC, OC, and SO₂**

T. Diehl et al.

Title Page

Abstract

Introduction

Conclusions

References

Tables

Figures



Back

Close

Full Screen / Esc

Printer-friendly Version

Interactive Discussion



3 regions. This effect might be due to relative large differences in the OC emission factors for certain combustion processes prevalent in these regions. Considering that the updated OC emissions reported by Lu et al. (2011) for China and India are considerably higher than in A2-MAP-v1 and also higher than A2-ACCMIP (3.7 Tg from China and 2.4 Tg from India in 2005), the OC emissions within A2-MAP-v1 over these regions seem to be underestimated.

4.1.4 Global emissions

The global emissions of BC, OC, and SO₂ are shown in Fig. 5. Globally, SO₂ emissions decrease during the 1980s in A2-ACCMIP, but show strong fluctuations in A2-MAP-v2 and A2-MAP-v1 due to the emission variability over the former USSR and Eastern Europe, respectively. There is an overall decrease during the 1990s, reflecting the strong reductions in emissions over the former USSR, Eastern Europe, the USA, and OECD Europe, which dominate during these years. After 2000, the surge of emissions over China and India dominate over further reductions in the other regions. After 1995, A2-MAP-v1 has the largest emissions, which is associated with the overestimated Eastern European emissions, as previously discussed. A2-ACCMIP has the lowest emissions of all 3 inventories. The differences among the inventories are up to 20 %, not counting the overestimated A2-MAP-v1 period.

Despite a strong intra-decadal variability of the A2-MAP-v1 BC emissions, both inventories agree within about 6 %. The overall trend is upward, interrupted by a sharp decrease in A2-MAP-v1 associated with the former USSR emissions around 1990, and another decrease from 1995 to 1996 associated with East Asia and the USA. After 2000, the global emission trend is clearly dominated by the Asian emissions increases.

Unlike BC, the OC emissions have an overall upwards trend which is similar for both inventories, with less intra-decadal variability in A2-MAP-v1. However, the agreement is worse (only within about 37 % to 52 %) due to the low OC emissions in A2-MAP-v1. The global trend is dominated for almost the whole period by the growth in East and South Asia, and is only briefly interrupted by a slight decrease around 1990 (due to the

**Anthropogenic,
biomass burning, and
volcanic emissions of
BC, OC, and SO₂**

T. Diehl et al.

Title Page

Abstract

Introduction

Conclusions

References

Tables

Figures

⏪

⏩

◀

▶

Back

Close

Full Screen / Esc

Printer-friendly Version

Interactive Discussion



massive decline over the former USSR) and again from 1995 to 1996 due to a decline over all regions except South Asia.

The two Hovmoeller diagrams in Fig. 6 depict the temporal variation of SO₂ emissions as a function of longitude in a compact form (in kg m⁻² d⁻¹) for A2-ACCMIP (Fig. 6, top) and for A2-MAP-v2 (Fig. 6, bottom). Both panels are for the Northern Hemisphere only, which contains most of the world's anthropogenic emissions. The strongest emissions in the USA are over the eastern part (centered around 80° W), with additional emissions occurring over the Midwestern USA around 90° W. Emissions over the Western USA seem to be rather low. All USA emissions decline over time. OECD Europe emissions are centered around 0°, transitioning into Eastern Germany at 10° E, followed by Eastern Europe and then the Ukraine at 25° E, emissions in Western Russia at 38° E, and Russian emissions near the Ural at 60° E. All these emissions decline as well. India at around 80° E starts to emit noticeable amounts in the late 1990s. Its emissions remain moderate even in 2005, as compared to emissions from China or emissions from other regions in the 1980s. China between 110° E and 120° E is the most powerful SO₂ emitting region by the early 1990s, and continues to increase up to 2005. One can also clearly see the emission differences of the two inventories for each region.

4.2 Ship emissions

Global SO₂ emissions from international ship traffic (Fig. 7) differ between A2-ACCMIP and A2-MAP-v1 by about 28 % in 1980, and converge to close agreement in 2005, with both inventories showing a strong increase after 1995. After 1995 they diverge, since A2-ACCMIP seems to assume a decrease of fuel sulfur content, causing a decline in emissions. The A2-MAP-v2 SO₂ emissions (based on Edgar v4.1) show a rather different temporal pattern, with a decline in the early 1980s, and a relative slow growth after 1995 as compared to the other inventories, resulting in about 85 % less SO₂ in emissions in 2005.

Anthropogenic, biomass burning, and volcanic emissions of BC, OC, and SO₂

T. Diehl et al.

Title Page

Abstract

Introduction

Conclusions

References

Tables

Figures

⏪

⏩

◀

▶

Back

Close

Full Screen / Esc

Printer-friendly Version

Interactive Discussion



OC ship emissions exhibit the closest agreement of all 3 species between A2-ACCMIP and A2-MAP-v1, and are within 10 % of each other, with even closer agreement after 1995.

There is less agreement between A2-ACCMIP and A2-MAP-v1 for the BC emissions, with a factor of 2 difference in 1980, which increases after 1995 due to the rapid growth of A2-ACCMIP. Within A2-MAP-v1, BC has the lowest growth rate of all 3 species after 1995. Different assumptions about the ship BC emission factor in the two inventories might be the cause for this discrepancy.

It should be noted that the ship emissions from A2-ACCMIP and A2-MAP-v1 are not completely independent. A2-MAP-v1 is based on Eyring et al. (2005a), while A2-ACCMIP is based on the mean of 3 different studies, including Eyring et al. (2005a), as described in Eyring et al. (2010).

4.3 Aircraft emissions

Global annual A2-ACCMIP black carbon emissions from air traffic are lower than A2-MAP emissions by about a factor of 1.6 for years prior to 2000, and increasingly lower for subsequent years (Fig. 8, top left). Estimates for years after 1999/2000 are based on interpolation to scenarios in both cases (2015 for A2-MAP, 2005 and 2010 for A2-ACCMIP), which are associated with higher uncertainties, providing a possible explanation for the larger discrepancy in these years. The jump in the A2-MAP data in 1983/1984, 1991/1992, and 1998/1999 is due to a combination of the height-dependency of the black carbon EI and changes in the vertical distribution of air traffic. The AEAP/UEET snapshot datasets for 1976, 1984, 1992, and 1999 have different vertical distributions of burned fuel, with later years having a higher fraction of fuel burned in higher altitudes (not shown). Since the black carbon EI we are using (Table 2) decreases with altitude until it reaches its minimum at 11.5 km, this temporarily reduces the BC emissions, even though the fuel amount is increasing. Except for these jumps, the increase of the global emissions is linear, and does not reflect air traffic changes in individual years due to events such as the 2001 terrorist attacks or the Gulf war in

**Anthropogenic,
biomass burning, and
volcanic emissions of
BC, OC, and SO₂**

T. Diehl et al.

Title Page

Abstract

Introduction

Conclusions

References

Tables

Figures



Back

Close

Full Screen / Esc

Printer-friendly Version

Interactive Discussion



1990/91. In a future version of the inventory, events like these could be represented by scaling the inventory with the global fuel production data from the IEA for this year, although this would not take into account the regional character of such events.

The A2-MAP inventory also includes a seasonal variation and emissions of SO₂, SO₄, and OC (Fig. 8, top right). The emission peak occurs in the NH summer (July/August), corresponding to typical vacation times. The SO₂ and SO₄ emissions decline after about 2005 due to the decreasing sulfur content of fuel, as described in Sect. 5.1.

Zonally averaged BC emission rates in kgm⁻³s⁻¹ for 1999 are shown in Fig. 8 (bottom left) and Fig. 8 (bottom right) for A2-ACCMIP and A2-MAP, respectively. A2-ACCMIP has 3 distinct emission altitudes at 3.5 km, 6.5 km, and a maximum within the typical cruise altitude band of 9–13 km (where aircraft spend most of their time) at about 10.7 km. The maximum of aircraft emissions in A2-MAP occurs at higher altitudes, with an emission peak at about 11.6 km, although this might also be attributed in parts to different assumptions about the EI of BC. The area below 9.5 km seems to be more transient, with no distinguished levels. Emissions in A2-MAP above 12.5 km are from the Concorde.

4.4 Volcanic emissions

In Fig. 9 (top) the location of the volcanoes included in our inventory are shown. Most volcanoes occur along tectonic plate boundaries where subduction, i.e. the convergence of plates, creates rising plumes of magma. They are also classified as arc volcanoes. Volcanoes formed by diverging tectonic plates, like in Iceland, are rift volcanoes. The volcanoes that do not occur along plate boundaries are the result of localized asthenosphere hot spots that melt through the Earth's crust. For example, the Hawaiian Island chain of volcanoes was created by a hot spot. Rift and hot spot volcanoes fall under the category of non-arc volcanoes. Generally, arc volcanoes are more explosive, with their magma having a higher viscosity and less SO₂ content, and they display a larger variation of SO₂ emission. Some of them are effusive emitters. Non-arc

**Anthropogenic,
biomass burning, and
volcanic emissions of
BC, OC, and SO₂**

T. Diehl et al.

Title Page

Abstract

Introduction

Conclusions

References

Tables

Figures

⏪

⏩

◀

▶

Back

Close

Full Screen / Esc

Printer-friendly Version

Interactive Discussion



volcanoes, on the other hand, erupt magma with a higher content of SO₂, show less variation in their SO₂ emissions, are generally not explosive, emit effusively, and have less frequent, but longer lasting eruptions. Both arc and non-arc volcanoes can be quietly degassing.

5 The time series of global annual volcanic A2-MAP SO₂ emissions from 1979 to 2009 is shown in Fig. 9 (bottom). The emissions range from about 22 Tgyr⁻¹ to 52 Tgyr⁻¹ (in 1991), while the median is about 26 Tgyr⁻¹. The largest peaks are due to El Chichon in 1982, Pinatubo in June 1991 (18 Tg), and Miyakejima from about 2001–2002. On average, about 12 Tg SO₂ are from quiescent degassing. The largest emissions from
10 quasi-continuous eruptions are from Etna in Sicily with about 45 Tg over the period 1979–2009.

4.5 Biomass burning emissions

ACCMIP “snapshot” biomass burning emissions were computed as averages from A2-ACCMIP emissions for the periods 1980–1989, 1990–1999, and 1997–2006, and were
15 labeled as ACCMIP “1980”, “1990”, and “2000” emissions. This procedure was applied for every month. However, due to the averaging procedure it seems more appropriate to place the snapshots in the middle of the corresponding periods, as shown in Fig. 10 of global biomass burning emissions. A2-ACCMIP data for 2010 is from the RCP8.5 scenario and the A2-ACCMIP 2009 data is identical to 2010. A2-MAP-v1 and
20 A2-MAP-v2 are identical in case of biomass burning for all 3 species. In order to enable a comparison between the A2-ACCMIP and A2-MAP inventories, we applied the emission factors (EF) described in Sect. 5.2 to A2-MAP.

4.5.1 Global emissions

Both the A2-MAP and A2-ACCMIP emissions display a strong inter-annual variability,
25 consistent with the nature of biomass burning, which is influenced by various yearly varying anthropogenic and natural factors. For example, the large peaks in 1997 and

**Anthropogenic,
biomass burning, and
volcanic emissions of
BC, OC, and SO₂**

T. Diehl et al.

Title Page

Abstract

Introduction

Conclusions

References

Tables

Figures

⏪

⏩

◀

▶

Back

Close

Full Screen / Esc

Printer-friendly Version

Interactive Discussion



1998 were caused by the combination of a drought induced by an extremely strong El Niño-Southern Oscillation (ENSO) event and human impacts on land-use in Indonesia, Malaysia, and Papua New Guinea. Globally, the A2-MAP emissions are significantly larger than the A2-ACCMIP emissions by a factor of about 1.5 to 2.5. BC emissions range from about 1.8 to 3.6 Tgyr⁻¹ for A2-ACCMIP and from 4.6 to 7 Tgyr⁻¹ for A2-MAP, while OC emissions range from 14 to 33 Tgyr⁻¹ for A2-ACCMIP and from 36 to 57 Tgyr⁻¹ for A2-MAP. The range of SO₂ emissions is from 2 to 6.6 Tgyr⁻¹ for A2-ACCMIP and from 5.4 to 8.4 Tgyr⁻¹ for A2-MAP. Since both datasets are based on GFEDv2 dry mass for years after 1996, the difference for these years is due only to different emission factors, where A2-MAP uses one global value, and A2-ACCMIP applies different regional values based on vegetation type. In addition to different magnitudes, the two datasets also differ with respect to the inter-annual variability pattern for years prior to 1997, where the two sets are based on different methodologies (Schultz et al., 2008; Duncan et al., 2003). Overall, A2-MAP emissions show less variability in this period than A2-ACCMIP emissions. This is caused by the African emissions, as discussed below.

4.5.2 Regional emissions

For a more detailed analysis of OC emissions (Fig. 12), we have specified six regions, covering the areas with the strongest biomass burning activities: South America (SAM), Northern Africa (NAF), Southern Africa (SAF), Southeast Asia (SEA), North America Boreal (NAB), and Europe Asia Boreal (EAB), see Fig. 11. For A2-MAP-v2, the fraction of global biomass burning emissions attributed to these 6 regions in 2005 is 87% for OC (Table 1), with the largest fraction originating from NAF and SAF (each 25%), followed by SAM with 19%. However, SEA can contribute over 30% in individual years. The boreal areas contribute the smallest fraction (about 5% combined).

Over SAM, A2-MAP emissions are higher than A2-ACCMIP for most years due to a higher emission factor. However, the RETRO burned dry mass (years prior to 1997) is higher than in Duncan et al. (2003) for some years, and in 1982 and 1992 even the

Anthropogenic, biomass burning, and volcanic emissions of BC, OC, and SO₂

T. Diehl et al.

Title Page

Abstract

Introduction

Conclusions

References

Tables

Figures



Back

Close

Full Screen / Esc

Printer-friendly Version

Interactive Discussion



**Anthropogenic,
biomass burning, and
volcanic emissions of
BC, OC, and SO₂**T. Diehl et al.

[Title Page](#)[Abstract](#)[Introduction](#)[Conclusions](#)[References](#)[Tables](#)[Figures](#)[Back](#)[Close](#)[Full Screen / Esc](#)[Printer-friendly Version](#)[Interactive Discussion](#)

emissions in A2-ACCMIP are larger than those in A2-MAP. Due to the lower dry mass before 1997, there is a pronounced increase in A2-MAP emissions after 1996. Emissions over SEA display a rather complex variation from year to year, with a higher A2-MAP emission factor again causing higher emissions for most years. Some years have higher dry mass burned or even higher emission values in A2-ACCMIP. The emissions (and dry mass burned) of A2-MAP over both African regions display no inter-annual variation up to 1996. This is described in Duncan et al. (2003) and attributed to a lack of information in these regions. The EF in A2-MAP is higher by about a factor of 2.3 in this region, causing higher A2-MAP emissions for all years. Dry mass in the two inventories differs between 17 % and 27 % before 1997. As already pointed out, the emissions in the boreal regions are generally lower than in the other regions, with the exception of 1998 emissions, caused by intense Siberian fires. EFs of the inventories are comparable over NAB and slightly higher in A2-MAP over EAB. The dry mass burned prior to 1997 is slightly higher in A2-MAP over EAB and comparable over NAB, with a few stronger events in A2-ACCMIP.

The two Hovmoeller diagrams in Fig. 13 show 4 main latitudinal bands of OC emissions and their temporal evolution from 1980 to 2005. There is an emission jump in the band centered around 10° S for A2-MAP (Fig. 13, top), associated with an increase of the dry mass burned over SAM, as mentioned above. The band around 3° S is the only band with occasional higher emissions in A2-ACCMIP (Fig. 13, bottom), occurring for the years 1982, 1987 and 1992. These events are associated with strong events in A2-ACCMIP over SEA. The major emission band of A2-MAP is located around 8° N, due to the consistently large emissions for all years in NAF. Although the emissions over SAF are comparable, they do not have the same impact in the Hovmoeller diagram, since the NAF emissions occur within a much thinner latitude band than the SAF emissions. Emissions in boreal regions after 1996 and therefore the EFs are comparable in both inventories. A2-MAP emissions are generally higher in prior years, and also extend further north. It should be noted that the same scale is used in both Hovmoeller diagrams, which makes emission peaks within A2-ACCMIP less visible.

Figure 14 shows the seasonal variation in the six regions. The seasonality of the two inventories is in close agreement in all regions. Biomass burning over SAM and SAF peaks in the SH dry season around September, while the maximum in NAF occurs during the NH winter. The peaks in both boreal regions occur in the NH summer. SEA does not have a well defined seasonal variation, because of our choice of the boundaries. This region contains a NH area approximately covering Thailand, Cambodia, Laos, Vietnam, and the Philippines, and also a SH area made up of Indonesia, Malaysia, Papua New Guinea, East Timor, and parts of Northern Australia. While the NH area has a burning peak in the NH spring, the SH area's burning maximum occurs in the SH dry season around September. In addition, the SH area is occasionally dominated by large burning events linked to ENSO-induced droughts, which further complicates the pattern.

5 Discussion

5.1 Calculation of aircraft emissions from fuel burned in A2-MAP

Jet fuel contains sulfur compounds, which are oxidized in the combustion process. We assume that all these oxides are emitted as SO_2 , although some direct emission of sulfur as SO_3 probably also occurs (Kärcher, 1999). Based on the fuel's average sulfur content, the emission index (EI) of SO_2 was estimated as $0.8 \text{ g}(\text{SO}_2) \text{ kg}(\text{fuel})^{-1}$ up to about 1999 (Sutkus, 2001). Future sulfur levels in jet fuel are expected to drop, with the EI of SO_2 decreasing to about 0.4 by 2015 (Sutkus, 2001). Hence we recommend to choose $\text{EI} = 0.8$ up to 1999, and then linearly interpolate the EI between 2000 and 2015. We do not take into account any variability of sulfur content by region.

Some measurements indicate that a small amount of SO_2 is converted to sulfate in the engine or in the near-field plume, and we use a number ratio of $\text{SO}_4/\text{SO}_2 = 0.5\%$, which corresponds to an engine power setting of about 50% (Petzold, 1998). The resulting effective EI is $\text{EI}_{\text{eff}}(\text{SO}_2) = \text{EI}(\text{SO}_2) \times 0.995$, and $\text{EI}_{\text{eff}}(\text{SO}_4) = \text{EI}(\text{SO}_2) \times 0.015$.

**Anthropogenic,
biomass burning, and
volcanic emissions of
BC, OC, and SO_2**

T. Diehl et al.

Title Page

Abstract

Introduction

Conclusions

References

Tables

Figures



Back

Close

Full Screen / Esc

Printer-friendly Version

Interactive Discussion



Other studies have found that this number ratio depends strongly on the type of engine, and report a range of 0.3 % to 4.5 % for an older engine and a value of about 3.3 % for a modern engine (Schumann et al., 2002).

Jet engines also emit black carbon (soot) particles, due to incomplete fuel combustion. We use EIs varying with altitude provided by Döpelheuer (2002), who used a correlation method taking into account different engine power settings, engine types, and flight levels. The derived values are representative of commercial aircraft in 1992, but we use them for all types of aircraft for all years, lacking additional information. The estimated EIs in $\text{g(BC) kg(fuel)}^{-1}$ and the corresponding altitudes in m are listed in Table 2. The global average of the EI is about $0.04 \text{ g(BC) kg(fuel)}^{-1}$. We would like to point out that the uncertainty of the black carbon EI is high due to a lack of data, particularly at climb altitudes, since the few available measurements have typically been undertaken at either ground level or cruise altitudes.

Studies by, e.g. Petzold (1998) suggest that some hydrocarbon compounds are emitted together with BC, and that about 75 % of the total carbon is emitted as BC at a power setting of 50 %. Based on these findings, we emit OC as $\text{OC} = 1/3 \times \text{BC}$, distributed into the same vertical levels as BC.

Initially, BC is emitted as hydrophobic aerosol. However, the soot particles probably become hydrophilic by interaction with H_2O and water-soluble species in the plume (Karcher, 1999). We therefore recommend emitting both BC and OC as hydrophilic, assuming that OC undergoes a similar transformation process.

5.2 Emission factors for biomass burning in A2-MAP

In A2-MAP, only DM is provided and not the actual emissions, so that modelers have to apply their own choice of emission factors (in units of $\text{g(species) kg(DM)}^{-1}$) for BC, OC, and SO_2 to obtain the corresponding biomass burning emissions. There are large ranges of emission factors used in the literature, see for example the recent study of Petrenko et al. (2012), and references therein. The most commonly used emission factors are those from the review paper of Andreae and Merlet (2001). These values depend

Anthropogenic, biomass burning, and volcanic emissions of BC, OC, and SO_2

T. Diehl et al.

Title Page

Abstract

Introduction

Conclusions

References

Tables

Figures

⏪

⏩

◀

▶

Back

Close

Full Screen / Esc

Printer-friendly Version

Interactive Discussion



**Anthropogenic,
biomass burning, and
volcanic emissions of
BC, OC, and SO₂**T. Diehl et al.

[Title Page](#)[Abstract](#)[Introduction](#)[Conclusions](#)[References](#)[Tables](#)[Figures](#)[Back](#)[Close](#)[Full Screen / Esc](#)[Printer-friendly Version](#)[Interactive Discussion](#)

on the vegetation type and are as follows: savanna and grassland, 0.48 g kg⁻¹ for BC, 3.4 g kg⁻¹ for OC, and 0.35 g kg⁻¹ for SO₂; tropical forest, 0.66 g kg⁻¹ for BC, 5.2 g kg⁻¹ for OC, and 0.57 g kg⁻¹ for SO₂; extratropical forest, 0.56 g kg⁻¹ for BC, 8.6–9.7 g kg⁻¹ for OC, and 1.0 g kg⁻¹ for SO₂. Another set of emission factors is provided in the Global Land Cover (GLC) database for 19 GLC vegetation types (Lioussé et al., 2003; Michel et al., 2005), and in the Global Fire Emissions Database version 3 (GFED3, van der Werf et al., 2010). In this paper, we have applied the emission factor for SO₂ used by Chin et al. (2002): EF(SO₂) = 1.12 g kg⁻¹. For BC and OC, we follow Chin et al. (2007) and use EF(BC) = 1.0 g kg⁻¹ and EF(OC) = 8.0 g kg⁻¹.

5.3 Injection heights

5.3.1 Anthropogenic emissions

In A2-ACCMIP and for SO₂ in A2-MAP-v2, the land-based anthropogenic emissions are stratified by sector. In this case, we recommend to evenly distribute the SO₂ emissions from the power (energy) sector into the levels between 100 m and 500 m above ground, and to inject all other sector emissions into the level(s) located within the first 100 m above ground. Power plants with high stacks tend to burn out the emissions and do not emit much BC and OC. For A2-MAP-v1 as well as for the ship emissions, the emissions should be also injected into the level(s) within the first 100 m.

5.3.2 Biomass burning emissions

Determining the top height H_p of plumes generated by wild-land fires and the distribution of emissions within the plume is a subject of ongoing research, and approaches of varying complexity have been explored. Statistical analysis of smoke plume heights suggests that the bulk of fire smoke stays in the atmospheric boundary layer, with 4–12 % of smoke plumes directly being injected above the boundary layer in the extratropics and about 4 % in the tropics (Val Martín et al., 2010), so the simplest approach

is to evenly distribute all the emissions into the model levels located within the boundary layer. However, occasionally strong fires in connection with favorable atmospheric conditions can send plumes into the free troposphere and even into the stratosphere (Freitas et al., 2007), especially in the case of boreal forest fires. Accordingly, H_p could be chosen according to geographical location. Several studies have used 2 km as the default (Lioussé et al., 1996), and 5–8 km for episodic intense boreal wildfires (Westphal and Toon, 1991), or 2–3 km for average boreal fires (Lavoue et al., 2000). Dentener et al. (2006) provide a table with emission fractions injected into 6 altitude bands for 4 regions. At the next level of complexity, one can try to calculate H_p from fire characteristics and atmospheric conditions, like the fire radiative power (FRP, Wooster et al., 2005), the atmospheric boundary layer (BL) height, and the Brunt-Vaisala frequency. For example, Sofiev et al. (2012a) provide such a formula for H_p . Val Martin et al. (2010) showed that stronger fires (larger FRP) will inject smoke above the BL; if there is a layer of relative stability in the free troposphere, the smoke will concentrate in it, otherwise H_p will be defined by the energy of the fire. Faint plumes will stay in the boundary layer. But the quantitative constraints for these processes are yet to be explored.

The approach of Sofiev et al. (2012a) has recently been used for the computation of injection height profiles for different regions (Sofiev et al., 2012b, data available on <http://is4fires.fmi.fi/>). The dataset is provided as monthly averages with a horizontal resolution of 1° , and a vertical resolution of 500 m. It also distinguishes between the night- and day-time combustion regimes and meteorological conditions.

The most complex approach currently is embedding a 1-D plume rise model within the CTM or GCM to explicitly calculate the vertical transport of hot gases and particles from fire events. Such a 1-D model is described in Freitas et al. (2007), for example.

5.3.3 Volcanic emissions

Since the volcano inventory is constructed such that the plume height is identical to the elevation of the volcano in case of non-eruptive degassing, the SO_2 emission should

**Anthropogenic,
biomass burning, and
volcanic emissions of
BC, OC, and SO_2**

T. Diehl et al.

Title Page

Abstract

Introduction

Conclusions

References

Tables

Figures



Back

Close

Full Screen / Esc

Printer-friendly Version

Interactive Discussion



be placed only in the model level which contains the crater elevation in this case. For all other cases, the emission should be injected into some fraction of the levels located within the plume. We recommend to evenly distribute the SO₂ emission among the model levels located within the top third of the plume, as outlined in Chin et al. (2000).

5.4 SO₂ specific recommendations

Following Chin et al. (2000), we recommend to apply a seasonal variation to the annual SO₂ land-based emission data over Europe, such that the fraction of the annual SO₂ assigned to the seasons is as follows: 0.325 for the winter months (December, January, February), 0.25 for spring (March, April, May), 0.175 for summer (June, July, August), and 0.25 for fall (September, October, November). Also, some fraction of sulfur should be directly emitted as SO₄. We recommend using 5 % over Europe and 3 % elsewhere.

5.5 Uncertainties

Globally, OC emissions are dominated by biomass burning (BB), SO₂ emissions are dominated by land-based anthropogenic (LBA) emissions, and BC emissions are influenced about equally by both of these sectors. The fraction which each of the sources contributes to the global total emissions in the A2-MAP inventory for the year 2005 are (Table 1): 50 % of BC from LBA, and 50 % from BB; 17 % of OC from LBA, and 82 % from BB; 73 % of SO₂ from LBA, 4 % from BB, 17 % from volcanoes, and 5 % from ship emissions. On a global basis, aircraft emissions contribute less than 1 % of the LBA emissions for each of the species, and BC and OC ship emissions contribute about 1 % to their respective global LBA emissions. Aircraft emissions are included in the inventories despite their small contribution to the global budget, because aircraft are the only source injecting BC, OC, and SO₂ continuously into the free troposphere, complemented by episodic BB events or sporadic volcanic eruptions. For years with major volcanic eruptions, the fraction of SO₂ emitted by LBA and BB sources would be lower than the values given for 2005.

Anthropogenic, biomass burning, and volcanic emissions of BC, OC, and SO₂

T. Diehl et al.

Title Page

Abstract

Introduction

Conclusions

References

Tables

Figures



Back

Close

Full Screen / Esc

Printer-friendly Version

Interactive Discussion



**Anthropogenic,
biomass burning, and
volcanic emissions of
BC, OC, and SO₂**

T. Diehl et al.

Title Page

Abstract

Introduction

Conclusions

References

Tables

Figures



Back

Close

Full Screen / Esc

Printer-friendly Version

Interactive Discussion



Bond et al. (2004) and Smith et al. (2011) estimated uncertainty ranges of BC/OC and SO₂ emissions, respectively. Based on these studies, uncertainties in regional emissions can be a factor of 2 or even larger. The uncertainty of global anthropogenic SO₂ emissions could be as high as a factor of 1.3. BC and OC uncertainties are generally higher than SO₂ uncertainties because SO₂ emissions are mainly dependent on fuel sulfur content and activity rates, while BC and OC emissions depend on combustion conditions. For BC and OC, the uncertainty estimates of biomass burning emissions are larger than those for anthropogenic emissions. Since most of OC is released by biomass burning, as shown in Table 1, the overall uncertainty of OC emissions is expected to be higher than the uncertainty of BC emissions. The differences of total emissions in Table 1 between A2-MAP-v2 and A2-ACCMIP are 34 % for BC, 46 % for OC, and 13 % for SO₂ (calculated without volcanic emissions), which falls in the expected range. For the global LBA emissions, the differences are 2 % for BC, 43 % for OC, and 17 % for SO₂. Biomass burning emissions all vary by a factor of 2 as a result of the different choice of emission factors, as discussed in Sect. 4.5.

The anthropogenic emission differences between A2-MAP-v2 and A2-ACCMIP vary substantially across regions and different years. The smallest deviations among the inventories occur for the USA and OECD Europe, where differences are within 20 %–30 % or even lower (for all species). The relative good agreement is probably due to accurate reporting of activities in these regions, and also to continuous measurements of power plant SO₂ emissions in case of the USA (Continuous Emission Monitoring Systems, CEMS). In Eastern Europe, SO₂ varies by up to 50 %, but mostly within 20 %–30 %. BC differences reach almost 100 % in some years, while OC differences range from 10 % to 30 %. The worst agreement occurs for the former USSR, where all 3 species vary frequently by up to 100 % between the two datasets, and even more in the case of OC. The reason for this strong disagreement remains unclear. Differences of SO₂ for South Asia as well as East Asia can reach up to 40 %, but are mostly below 20 %. South Asian BC and OC emissions vary by up to 25 % among the inventories. Over East China, the agreement is within 15 % for BC, and between 30–60 % for OC.

It should be noted that large differences between A2-MAP and A2-ACCMIP for some years between decadal endpoints might be overemphasized, if A2-MAP exhibits a strong variability during this decade, which is not represented in A2-ACCMIP due to the linear interpolation.

In their recent analysis of 13 global biomass burning estimates, Petrenko et al. (2012) found that burned dry mass varied globally by a factor of 4, and even more in some regions. Emission factors varied by up to about a factor of 2 in tropical regions, but showed less variation in boreal regions. As discussed in Sect. 4.5, the biomass burning emission differences of A2-MAP and A2-ACCMIP are only caused by different choices of the EF for years after 1996. The EF for OC varies from about a factor of 1 in the boreal regions to 2.3 in Africa, leading to emission differences of up to 100 %. For years prior to 1997, the dry mass differences are typically below 100 %, with the exception of the EAB region, where some deviations up to the factor of 4 reported by Petrenko et al. (2012) occur.

Regarding ship emissions, we would like to note that the accuracy of “top-down” ship emission inventories, where global speciated emissions are distributed via spatial proxies, is generally less accurate in coastal areas as compared to the open ocean, since the fraction of smaller ships, which participate less frequently in reporting ship location data, is higher in these areas. It might be more appropriate to use a “bottom-up” approach here, i.e. an approach which relies on local ship- and route-specific emissions.

6 Summary and conclusions

In this paper we have presented and compared two emission inventories of BC, OC, and SO₂ from anthropogenic sources, biomass burning and volcanoes for the period 1980–2010. The overall goal was to provide choices of emission databases for aerosol hindcast studies, and some guidance on how to apply them in model experiments. We discussed approaches how to compute injection heights and (for A2-MAP) emission factors and emission indices.

Anthropogenic, biomass burning, and volcanic emissions of BC, OC, and SO₂

T. Diehl et al.

Title Page

Abstract

Introduction

Conclusions

References

Tables

Figures



Back

Close

Full Screen / Esc

Printer-friendly Version

Interactive Discussion



Anthropogenic, biomass burning, and volcanic emissions of BC, OC, and SO₂

T. Diehl et al.

Title Page

Abstract

Introduction

Conclusions

References

Tables

Figures



Back

Close

Full Screen / Esc

Printer-friendly Version

Interactive Discussion



Both datasets capture the general trends of decreasing emissions over the USA and OECD Europe since 1980 and since about 1990 over the former USSR and Eastern Europe, and of increasing emissions over South and East Asia, particularly since 2000. Global differences between the two inventories fall within the range of uncertainty estimates in the literature, with SO₂ showing the smallest difference. For individual regions, the variation is generally larger. The highest differences occur over the former USSR, where OC differs by more than 100 % among the inventories.

Globally, the highest differences occur for biomass burning emissions, which vary by a factor of 2 for years after 1996 due to a higher emission factor applied to A2-MAP. Differences of dry mass burned for years up to 1996 vary significantly according to region and year, and are larger than 100 % in some cases.

The two inventories differ in various aspects and the modeler's selection depends on the focus and requirements of the hindcast study. The inter-annual variability of A2-MAP anthropogenic emissions is based on reported activity data, while A2-ACCMIP data was generated via linear interpolation between decadal endpoints. A2-ACCMIP should be chosen if consistency with CMIP5 or ACCMIP simulations is required. The horizontal resolution of A2-ACCMIP is 0.5° × 0.5°, compared to 1.0° × 1.0° for A2-MAP. A2-ACCMIP data is available up to 2010 for all emissions, while A2-MAP data ends in 2007 for anthropogenic and biomass burning emissions. However, A2-ACCMIP contains data from projected emissions from the RCP8.5 scenario for years after 2000. Only A2-MAP contains volcanic emissions.

Both A2-MAP and A2-ACCMIP were constructed by combining data from multiple inventories and thus have internal inconsistencies to some degree, but it is not clear how important these are. For example, the trend of BC in A2-MAP-v1 and the trend of SO₂ in A2-MAP-v2 might be different in a region for a given period just because different population growth data was used for the two versions.

Future improvements include updating the A2-MAP inventory with more recent data on a region-by-region basis, starting with China and India, which will be updated with the emissions developed by Lu et al. (2011). Volcanic emissions should be updated

with eruptions from 2010 and 2011. The crucial role of emission factors became apparent, and their uncertainty must be further reduced by lab and/or field measurements, specifically for wildland fires. The temporal resolution should be increased to include seasonality for anthropogenic emissions, at least for mid-latitude regions and regions where travel patterns vary significantly throughout the year. Finally, inverse modeling methods should be applied to provide independent emission datasets based on satellite retrievals of AOD, which could help to constrain the uncertainty range of the emission estimates.

Acknowledgements. The authors would like to thank T. Bond for providing gridded land-based anthropogenic emissions of BC and OC. AEAP/UEET datasets containing burned fuel from air traffic were kindly made available by S. Baughcum. We would like to thank L. Siebert for providing data on volcanic eruptions. T. D., M. C., and D. S. would like to acknowledge support received from NASA's MAP program.

References

- Andreae, M. O. and Merlet, P.: Emission of trace gases and aerosols from biomass burning, *Global Biogeochem. Cy.*, 15, 955–966, doi:10.1029/2000GB001382, 2001.
- Andres, R. J. and Kasgnoc, A. D.: A time-averaged inventory of subaerial volcanic sulfur emissions, *J. Geophys. Res.*, 103, 25251–25261, doi:10.1029/98JD02091, 1998.
- Baughcum, S. L., Henderson, S. C., and Tritz, T. G.: Scheduled Civil Aircraft Emission Inventories for 1976 and 1984: Database Development and Analysis, Contractor Report 4722, National Aeronautics and Space Administration, Hampton, VA, USA, 157 pp., 1996a.
- Baughcum, S. L., Tritz, T. G., Henderson, S. C., and Pickett, D. C.: Scheduled Civil Aircraft Emission Inventories for 1992: Database Development and Analysis, Contractor Report 4700, National Aeronautics and Space Administration, Hampton, VA, USA, 216 pp., 1996b.
- Baughcum, S. L., Sutkus, D. J., and Henderson, S. C.: Year 2015 Aircraft Emission Scenario for Scheduled Air Traffic, Contractor Report 1998–207638, National Aeronautics and Space Administration, Hampton, VA, USA, 52 pp., 1998.
- Berresheim, H. and Jaeschke, W.: The contribution of volcanoes to the global atmospheric sulfur budget, *J. Geophys. Res.*, 88, 3732–3740, doi:10.1029/JC088iC06p03732, 1983.

Anthropogenic, biomass burning, and volcanic emissions of BC, OC, and SO₂

T. Diehl et al.

Title Page

Abstract

Introduction

Conclusions

References

Tables

Figures



Back

Close

Full Screen / Esc

Printer-friendly Version

Interactive Discussion



Anthropogenic, biomass burning, and volcanic emissions of BC, OC, and SO₂

T. Diehl et al.

Title Page

Abstract

Introduction

Conclusions

References

Tables

Figures

⏪

⏩

◀

▶

Back

Close

Full Screen / Esc

Printer-friendly Version

Interactive Discussion



- Blake, S.: Correlations between eruption magnitude, SO₂ yield, and surface cooling, in: Volcanic Degassing, Special Publication of the Geological Society of London No. 213, edited by: Oppenheimer, C., Pyle, D. M., and Barclay, J., Geological Society, London, UK, 177–202, 2003.
- 5 Bond, T. C., Streets, D. G., Yarber, K. F., Nelson, S. M., Woo, J.-H., and Klimont, Z.: A technology-based global inventory of black and organic carbon emissions from combustion, *J. Geophys. Res.*, 109, D14203, doi:10.1029/2003JD003697, 2004.
- Carn, S. A., Krueger, A. J., Bluth, G. J. S., Schaefer, S. J., Krotkov, N. A., Watson, I. M., and Datta, S.: Volcanic eruption detection by the Ozone Mapping Spectrometer (TOMS) instruments: a 22-year record of sulphur dioxide and ash emissions, in: Volcanic Degassing, Special Publication of the Geological Society of London No. 213, edited by: Oppenheimer, C., Pyle, D. M., and Barclay, J., Geological Society, London, UK, 177–202, 2003.
- 10 CCSP 2009: Atmospheric Aerosol Properties and Climate Impacts, a Report by the US Climate Change Science Program and the Subcommittee on Global Change Research, edited by: Chin, M., Kahn, R. A., and Schwartz, S. E., National Aeronautics and Space Administration, Washington, D.C., USA, 128 pp., 2009.
- 15 Chin, M., Rood, R. B., Lin, S.-J., Müller, J.-F., and Thompson, A. M.: Atmospheric sulfur cycle simulated in the global model GOCART: model description and global properties, *J. Geophys. Res.*, 105, 24671–24687, doi:10.1029/2000JD900384, 2000.
- 20 Chin, M., Ginoux, P., Kinne, S., Torres, O., Holben, B. N., Duncan, B. N., Martin, R. V., Logan, J. A., Higurashi, A., and Nakajima, T.: Tropospheric aerosol optical thickness from the GOCART model and comparisons with satellite and sun photometer measurements, *J. Atmos. Sci.*, 59, 461–483, 2002.
- Chin, Mian, Diehl, T., Ginoux, P., and Malm, W.: Intercontinental transport of pollution and dust aerosols: implications for regional air quality, *Atmos. Chem. Phys.*, 7, 5501–5517, doi:10.5194/acp-7-5501-2007, 2007.
- 25 Christian, T. J., Kleiss, B., Yokelson, R. J., Holzinger, R., Crutzen, P. J., Hao, W. M., Sahaarjo, B. H., and Ward, D. E.: Comprehensive laboratory measurements of biomass-burning emissions: 1. Emissions from Indonesian, African, and other fuels, *J. Geophys. Res.*, 108, 4719, doi:10.1029/2003JD003704, 2003.
- 30 Dentener, F., Kinne, S., Bond, T., Boucher, O., Cofala, J., Generoso, S., Ginoux, P., Gong, S., Hoelzemann, J. J., Ito, A., Marelli, L., Penner, J. E., Putaud, J.-P., Textor, C., Schulz, M., van der Werf, G. R., and Wilson, J.: Emissions of primary aerosol and precursor gases in

Anthropogenic, biomass burning, and volcanic emissions of BC, OC, and SO₂

T. Diehl et al.

Title Page

Abstract

Introduction

Conclusions

References

Tables

Figures

◀

▶

◀

▶

Back

Close

Full Screen / Esc

Printer-friendly Version

Interactive Discussion



the years 2000 and 1750 prescribed data-sets for AeroCom, *Atmos. Chem. Phys.*, 6, 4321–4344, doi:10.5194/acp-6-4321-2006, 2006.

Döpelheuer, A.: Application-Oriented Methods to Determine CO, HC and Soot from Aircraft Engines, Ph.D. Thesis, University of Bochum, Bochum, Germany, 2002.

5 Duncan, B. N., Martin, R., Staudt, A., Yevich, R., and Logan, J.: Interannual and seasonal variability of biomass burning emissions constrained by satellite observations, *J. Geophys. Res.*, 108, 4100, doi:10.1029/2002JD002378, 2003.

Eickhout, B., den Elzen, M. G. J., and Kreileman, G. J. J.: The Atmosphere-Ocean System of IMAGE 2.2. A global model approach for atmospheric concentrations, and climate and sea level projections, RIVM report 481508017, National Institute for Public Health and the Environment (RIVM), Bilthoven, The Netherlands, 2004.

European Commission: Joint Research Centre (JRC)/Netherlands Environmental Assessment Agency (PBL): Emission Database for Global Atmospheric Research (EDGAR), release version 4.1., available at: <http://edgar.jrc.ec.europa.eu> (last access: February 2011), 2010.

15 Eyring, V., Köhler, H. W., van Aardenne, J., and Lauer, A.: Emissions from international shipping: 1. the last 50 years, *J. Geophys. Res.*, 110, D17305, doi:10.1029/2004JD005619, 2005a.

Eyring, V., Köhler, H. W., Lauer, A., and Lemper, B.: Emissions from international shipping: 2. impact of future technologies on scenarios until 2050, *J. Geophys. Res.*, 110, D17306, doi:10.1029/2004JD005620, 2005b.

20 Eyring, V., Isaksen, I. S. A., Berntsen, T., Collins, W. J., Corbett, J. J., Endresen, O., Grainger, R. G., Moldanova, J., Schlager, H., and Stevenson, D. S.: Transport impacts on atmosphere and climate: shipping, *Atmos. Environ.*, 44, 4735–4771, doi:10.1016/j.atmosenv.2009.04.059, 2010.

25 Food and Agriculture Organization (FAO): World Reference Base (WRB) Map of World Soil Resources. Land and Water Development Division AGL, <http://www.fao.org/ag/agl/agll/wrb/soilres.stm>, last access: 16 February 2010, Food and Agriculture Organization of the United Nations, Rome, Italy, 2003.

30 Freitas, S. R., Longo, K. M., Chatfield, R., Latham, D., Silva Dias, M. A. F., Andreae, M. O., Prins, E., Santos, J. C., Gielow, R., and Carvalho Jr., J. A.: Including the sub-grid scale plume rise of vegetation fires in low resolution atmospheric transport models, *Atmos. Chem. Phys.*, 7, 3385–3398, doi:10.5194/acp-7-3385-2007, 2007.

Anthropogenic, biomass burning, and volcanic emissions of BC, OC, and SO₂

T. Diehl et al.

Title Page

Abstract

Introduction

Conclusions

References

Tables

Figures

⏪

⏩

◀

▶

Back

Close

Full Screen / Esc

Printer-friendly Version

Interactive Discussion

Granier, C., Bessagnet, B., Bond, T., D'Angiola, A., van der Gon, H. D., Frost, G. J., Heil, A., Kaiser, J. W., Kinne, S., Klimont, Z., Kloster, S., Lamarque, J.-F., Liousse, C., Masui, T., Meleux, F., Mieville, A., Ohara, T., Raut, J. C., Riahi, K., Schultz, M. G., Smith, S. J., Thompson, A., van Aardenne, J., van der Werf, G. R., and van Vuuren, D. P.: Evolution of anthropogenic and biomass burning emissions of air pollutants at global and regional scales during the 1980–2010 period, *Climatic Change*, 109, 163–190, doi:10.1007/s10584-011-0154-1, 2011.

Haywood, J. and Schulz, M.: Causes of the reduction in uncertainty in the anthropogenic radiative forcing of climate between IPCC (2001) and IPCC (2007), *Geophys. Res. Lett.*, 34, L20701, doi:10.1029/2007GL030749, 2007.

Hsu, N. C., Gautam, R., Sayer, A. M., Bettenhausen, C., Li, C., Jeong, M. J., Tsay, S.-C., and Holben, B. N.: Global and regional trends of aerosol optical depth over land and ocean using SeaWiFS measurements from 1997 to 2010, *Atmos. Chem. Phys. Discuss.*, 12, 8465–8501, doi:10.5194/acpd-12-8465-2012, 2012.

Huneus, N., Schulz, M., Balkanski, Y., Griesfeller, J., Prospero, J., Kinne, S., Bauer, S., Boucher, O., Chin, M., Dentener, F., Diehl, T., Easter, R., Fillmore, D., Ghan, S., Ginoux, P., Grini, A., Horowitz, L., Koch, D., Krol, M. C., Landing, W., Liu, X., Mahowald, N., Miller, R., Morcrette, J.-J., Myhre, G., Penner, J., Perlwitz, J., Stier, P., Takemura, T., and Zender, C. S.: Global dust model intercomparison in AeroCom phase I, *Atmos. Chem. Phys.*, 11, 7781–7816, doi:10.5194/acp-11-7781-2011, 2011.

IMAGE team: The IMAGE 2.2 implementation of the SRES scenarios. A comprehensive analysis of emissions, climate change and impacts in the 21st century, RIVM CD-ROM publication 481508018, National Institute for Public Health and the Environment (RIVM), Bilthoven, The Netherlands, 2001.

International Energy Agency (IEA): Energy Statistics of OECD Countries, Paris, France, 1998a. International Energy Agency (IEA): Energy Statistics of Non-OECD Countries, Paris, France, 1998b.

Forster, P., Ramaswamy, V., Artaxo, P., Berntsen, T., Betts, R., Fahey, D. W., Haywood, J., Lean, J., Lowe, D. C., Myhre, G., Nganga, J., Prinn, R., Raga, G., Schulz, M., and Dorland, R. V.: Changes in atmospheric constituents and in radiative forcing, in: *Climate Change 2007: The Physical Science Basis. Contribution of Working Group I to the Fourth Assessment Report of the Intergovernmental Panel on Climate Change*, edited by: Solomon, S.,

Anthropogenic, biomass burning, and volcanic emissions of BC, OC, and SO₂

T. Diehl et al.

[Title Page](#)
[Abstract](#)
[Introduction](#)
[Conclusions](#)
[References](#)
[Tables](#)
[Figures](#)




[Back](#)
[Close](#)
[Full Screen / Esc](#)
[Printer-friendly Version](#)
[Interactive Discussion](#)


- Qin, D., Manning, M., Chen, Z., Marquis, M., Averyt, K. B., Tignor, M., and Miller, H. L., Cambridge University Press, Cambridge, UK and New York, NY, USA, 2007.
- Kärcher, B.: Aviation-produced aerosols and contrails, *Surv. Geophys.*, 20, 113–167, 1999.
- Kinne, S., Schulz, M., Textor, C., Guibert, S., Balkanski, Y., Bauer, S. E., Bernsten, T., Berglen, T. F., Boucher, O., Chin, M., Collins, W., Dentener, F., Diehl, T., Easter, R., Feichter, J., Fillmore, D., Ghan, S., Ginoux, P., Gong, S., Grini, A., Hendricks, J., Herzog, M., Horowitz, L., Isaksen, I., Iversen, T., Kirkevåg, A., Kloster, S., Koch, D., Kristjansson, J. E., Krol, M., Lauer, A., Lamarque, J. F., Lesins, G., Liu, X., Lohmann, U., Montanaro, V., Myhre, G., Penner, J., Pitari, G., Reddy, S., Seland, O., Stier, P., Takemura, T., and Tie, X.: An AeroCom initial assessment – optical properties in aerosol component modules of global models, *Atmos. Chem. Phys.*, 6, 1815–1834, doi:10.5194/acp-6-1815-2006, 2006.
- Koch, D., Schulz, M., Kinne, S., McNaughton, C., Spackman, J. R., Balkanski, Y., Bauer, S., Bernsten, T., Bond, T. C., Boucher, O., Chin, M., Clarke, A., De Luca, N., Dentener, F., Diehl, T., Dubovik, O., Easter, R., Fahey, D. W., Feichter, J., Fillmore, D., Freitag, S., Ghan, S., Ginoux, P., Gong, S., Horowitz, L., Iversen, T., Kirkevåg, A., Klimont, Z., Kondo, Y., Krol, M., Liu, X., Miller, R., Montanaro, V., Moteki, N., Myhre, G., Penner, J. E., Perlwitz, J., Pitari, G., Reddy, S., Sahu, L., Sakamoto, H., Schuster, G., Schwarz, J. P., Seland, Ø., Stier, P., Takegawa, N., Takemura, T., Textor, C., van Aardenne, J. A., and Zhao, Y.: Evaluation of black carbon estimations in global aerosol models, *Atmos. Chem. Phys.*, 9, 9001–9026, doi:10.5194/acp-9-9001-2009, 2009.
- Koffi, B., Schulz, M., Bréon, F.-M., Griesfeller, J., Winker, D., Balkanski, Y., Bauer, S., Bernsten, T., Chin, M., Collins, W. D., Dentener, F., Diehl, T., Easter, R., Ghan, S., Ginoux, P., Gong, S., Horowitz, L. W., Iversen, T., Kirkevåg, A., Koch, D., Krol, M., Myhre, G., Stier, P., and Takemura, T.: Application of the CALIOP Layer Product to evaluate the vertical distribution of aerosols estimated by global models: Part 1. AeroCom phase I results, *J. Geophys. Res.*, 117, D10201, doi:10.1029/2011JD016858, 2012.
- Lamarque, J.-F., Bond, T. C., Eyring, V., Granier, C., Heil, A., Klimont, Z., Lee, D., Liousse, C., Mieville, A., Owen, B., Schultz, M. G., Shindell, D., Smith, S. J., Stehfest, E., Van Aardenne, J., Cooper, O. R., Kainuma, M., Mahowald, N., McConnell, J. R., Naik, V., Riahi, K., and van Vuuren, D. P.: Historical (1850–2000) gridded anthropogenic and biomass burning emissions of reactive gases and aerosols: methodology and application, *Atmos. Chem. Phys.*, 10, 7017–7039, doi:10.5194/acp-10-7017-2010, 2010.

**Anthropogenic,
biomass burning, and
volcanic emissions of
BC, OC, and SO₂**

T. Diehl et al.

[Title Page](#)[Abstract](#)[Introduction](#)[Conclusions](#)[References](#)[Tables](#)[Figures](#)[⏪](#)[⏩](#)[◀](#)[▶](#)[Back](#)[Close](#)[Full Screen / Esc](#)[Printer-friendly Version](#)[Interactive Discussion](#)

Lavoué, D., Liousse, C., Cachier, H., Stocks, B. J., and Goldammer, J. G.: Modeling of carbonaceous particles emitted by boreal and temperate wildfires at northern latitudes, *J. Geophys. Res.*, 105(D22), 26871–26890, doi:10.1029/2000JD900180, 2000.

Liousse, C., Penner, J. E., Chuang, C., Walton, J. J., Eddleman, H., and Cachier, H.: A global three-dimensional model study of carbonaceous aerosols, *J. Geophys. Res.*, 101, 19411–19432, doi:10.1029/95JD03426, 1996.

Liousse, C., Andreae, M. O., Artaxo, P., Barbosa, P., Cachier, H., Gregoire, J. M., Hobbs, P., Lavoue, D., Mouillot, F., Penner, J., Scholes, M., and Schultz, M. G.: Deriving global quantitative estimates for spatial and temporal distributions of biomass burning emissions, in: *IGAC Book on Emissions*, edited by: Granier, C., Artaxo P., and Reeves, C., Kluwer, The Netherlands, 2003.

Lloyd's Maritime Information System (LMIS): The Lloyd's Maritime Database (CD-ROM), Lloyd's Register–Fairplay Ltd., London, UK, 2002.

Robert, J., Keen, W., Logan, J., and Yevich, R.: Global chlorine emissions from biomass burning: reactive chlorine emissions inventory, *J. Geophys. Res.*, 104, 8373–8389, doi:10.1029/1998JD100077, 1999.

Lu, Z., Zhang, Q., and Streets, D. G.: Sulfur dioxide and primary carbonaceous aerosol emissions in China and India, 1996–2010, *Atmos. Chem. Phys.*, 11, 9839–9864, doi:10.5194/acp-11-9839-2011, 2011.

Michel, C., Liousse, C., Grégoire, J.-M., Tansey, K., Carmichael, G. R., and Woo, J.-H.: Biomass burning emission inventory from burnt area data given by the SPOT-VEGETATION system in the frame of TRACE-P and ACE-Asia campaigns, *J. Geophys. Res.*, 110, D09304, doi:10.1029/2004JD005461, 2005.

Mortlock, A. and Alstyne, R. V.: Military, Charter, Unreported Domestic Traffic and General Aviation 1976, 1984, 1992, and 2015 Emission Scenarios, Contractor Report 1998-207639, National Aeronautics and Space Administration, Hampton, VA, USA, 120 pp., 1998.

Newhall, C. G. and Self, S.: The volcanic explosivity index (VEI): an estimate of explosive magnitude for historical volcanism, *J. Geophys. Res.*, 87, 1231–1238, doi:10.1029/JC087iC02p01231, 1982.

Ohara, T., Akimoto, H., Kurokawa, J., Horii, N., Yamaji, K., Yan, X., and Hayasaka, T.: An Asian emission inventory of anthropogenic emission sources for the period 1980–2020, *Atmos. Chem. Phys.*, 7, 4419–4444, doi:10.5194/acp-7-4419-2007, 2007.

Anthropogenic, biomass burning, and volcanic emissions of BC, OC, and SO₂

T. Diehl et al.

[Title Page](#)
[Abstract](#)
[Introduction](#)
[Conclusions](#)
[References](#)
[Tables](#)
[Figures](#)




[Back](#)
[Close](#)
[Full Screen / Esc](#)
[Printer-friendly Version](#)
[Interactive Discussion](#)

- Olivier, J. G. J. and Berdowski, J. J. M.: Global emissions sources and sinks, in: The Climate System, edited by: Berdowski, J., Guicherit, R., and Heij, B. J., A.A. Balkema Publishers/Swets & Zeitlinger Publishers, Lisse, The Netherlands, 33–78, 2001.
- Olivier, J. G. J., van Aardenne, J. A., Dentener, F. J., Pagliari, V., Ganzeveld, L. N., and Peters, J. A. H. W.: Recent trends in global greenhouse gas emissions: regional trends 1970–2000 and spatial distribution of key sources in 2000, *Environ. Sci.*, 2, 81–99, doi:10.1080/15693430500400345, 2005.
- Penner, J. E., Quaas, J., Storelvmo, T., Takemura, T., Boucher, O., Guo, H., Kirkevåg, A., Kristjánsson, J. E., and Seland, Ø.: Model intercomparison of indirect aerosol effects, *Atmos. Chem. Phys.*, 6, 3391–3405, doi:10.5194/acp-6-3391-2006, 2006.
- Petrenko, M., Kahn, R., Chin, M., Soja, A., Kucsera, T., and Harshvardhan: The use of satellite-measured aerosol optical depth to constrain biomass burning emissions source strength in the global model GOCART, *J. Geophys. Res.*, doi:10.1029/2012JD017870, in press, 2012.
- Petzold, A. and Schröder, F. P.: Jet engine exhaust aerosol characterization, *Aerosol Sci. Technol.*, 28, 62–76, 1998.
- Petzold, A., Feldpausch, P., Fritzsche, L., Minikin, A., Lauer, P., and Bauer, H.: Particle emissions from ship engines, European Aerosol Conference, Budapest, Hungary, 6–10 September 2004, *J. Aerosol Sci.*, 35, 1095–1096, 2004.
- Randerson, J. T., van der Werf, G. R., Giglio, L., Collatz, G. J., and Kasibhatla, P. S.: Global Fire Emissions Database, Version 2 (GFEDv2.1), Data set, available at: <http://daac.ornl.gov/>, Oak Ridge National Laboratory Distributed Active Archive Center, Oak Ridge, Tennessee, USA, doi:10.3334/ORNLDAAC/849, 2007.
- Riahi, K., Rao, S., Krey, V., Cho, C., Chirkov, V., Fischer, G., Kindermann, G., Nakicenovic, N., and Rafaj, P.: RCP 8.5 – a scenario of comparatively high greenhouse gas emissions, *Climatic Change*, 109, 33–57, doi:10.1007/s10584-011-0149-y, 2011.
- Schnetzler, C. C., Bluth, G. J. S., Krueger, A. J., and Walter, L. S.: A proposed volcanic sulfur dioxide index (VSI), *J. Geophys. Res.*, 102, 20087–20091, doi:10.1029/97JB01142, 1997.
- Schultz, M. G., Backman, L., Balkanski, Y., Bjoerndalsaeter, S., Brand, R., Burrows, J. P., Dalseren, S., de Vasconcelos, M., Grodtmann, B., Hauglustaine, D. A., Heil, A., Hoelzemann, J. J., Isaksen, I. S. A., Kaurola, J., Knorr, W., Ladstaetter-Weißenmayer, A., Mota, B., Oom, D., Pacyna, J., Panasiuk, D., Pereira, J. M. C., Pulles, T., Pyle, J., Rast, S., Richter, A., Savage, N., Schnadt, C., Schulz, M., Spessa, A., Staehelin, J., Sundet, J. K., Szopa, S., Thonckicke, K., van het Bolscher, M., van Noije, T., van Velthoven, P., Vik, A. F., and Wittrock, F.:

**Anthropogenic,
biomass burning, and
volcanic emissions of
BC, OC, and SO₂**

T. Diehl et al.

Title Page

Abstract

Introduction

Conclusions

References

Tables

Figures

⏪

⏩

◀

▶

Back

Close

Full Screen / Esc

Printer-friendly Version

Interactive Discussion



REanalysis of the TROpospheric chemical composition over the past 40 years, a long-term global modeling study of tropospheric chemistry funded under the 5th EU framework programme, Reports on Earth System Science 48/2007, Max Planck Institute for Meteorology, Hamburg, Germany, available at: [http://www.mpimet.mpg.de/fileadmin/publikationen/](http://www.mpimet.mpg.de/fileadmin/publikationen/Reports/WEB_BzE_48.pdf)

5 Reports/WEB_BzE_48.pdf (last access: July 2012), 2007.
Schultz, M. G., Heil, A., Hoelzemann, J. J., Spessa, A., Thonicke, K., Goldammer, J., Held, A. C., Pereira, J. M., and van het Bolscher, M.: Global wildland fire emissions from 1960 to 2000, *Global Biogeochem. Cy.*, 22, GB2002, doi:10.1029/2007GB003031, 2008.

10 Schulz, M., Textor, C., Kinne, S., Balkanski, Y., Bauer, S., Bernsten, T., Berglen, T., Boucher, O., Dentener, F., Guibert, S., Isaksen, I. S. A., Iversen, T., Koch, D., Kirkevåg, A., Liu, X., Montanaro, V., Myhre, G., Penner, J. E., Pitari, G., Reddy, S., Seland, Ø., Stier, P., and Takemura, T.: Radiative forcing by aerosols as derived from the AeroCom present-day and pre-industrial simulations, *Atmos. Chem. Phys.*, 6, 5225–5246, doi:10.5194/acp-6-5225-2006, 2006.

15 Schulz, M., Chin, M., and Kinne, S.: The aerosol model comparison project, AeroCom, Phase II: clearing up diversity, *IGAC Newslett.*, 41, 2–11, 2009.

Schumann, U., Arnold, F., Busen, R., Curtius, J., Kärcher, B., Kiendler, A., Petzold, A., Schlager, H., Schröder, F., and Wohlfrom, K.-H.: Influence of fuel sulfur on the composition of aircraft exhaust plumes: the experiments SULFUR 1–7, *J. Geophys. Res.*, 107, 4247, doi:10.1029/2001JD000813, 2002.

20 Shindell, D. and Lamarque, J.-F.: Atmospheric chemistry & climate model intercomparison project (ACC-MIP), *IGAC Newslett.*, 41, 19–22, 2009.

Simkin, T., and Siebert, L.: Global Volcanism FAQs, Smithsonian Institution, Global Volcanism Program Digital Information Series, GVP-5, available at: <http://www.volcano.si.edu/education/questions/> (last access: August 2010), 2002.

25 Sinha, P., Hobbs, P. V., Yokelson, R. J., Christian, T. J., Kirchstetter, T. W., and Brientjes, R.: Emissions of trace gases and particles from two ships in the southern Atlantic Ocean, *Atmos. Environ.*, 37, 2139–2148, 2003.

Smith, S. J., van Aardenne, J., Klimont, Z., Andres, R. J., Volke, A., and Delgado Arias, S.: Anthropogenic sulfur dioxide emissions: 1850–2005, *Atmos. Chem. Phys.*, 11, 1101–1116, doi:10.5194/acp-11-1101-2011, 2011.

30 Sofiev, M., Ermakova, T., and Vankevich, R.: Evaluation of the smoke-injection height from wildland fires using remote-sensing data, *Atmos. Chem. Phys.*, 12, 1995–2006, doi:10.5194/acp-12-1995-2012, 2012a.

Anthropogenic, biomass burning, and volcanic emissions of BC, OC, and SO₂

T. Diehl et al.

[Title Page](#)
[Abstract](#)
[Introduction](#)
[Conclusions](#)
[References](#)
[Tables](#)
[Figures](#)




[Back](#)
[Close](#)
[Full Screen / Esc](#)
[Printer-friendly Version](#)
[Interactive Discussion](#)


- Sofiev, M., Vankevich, R., Ermakova, T., and Hakkarainen, J.: Global mapping of vertical injection profiles of wild-fire emission, *Atmos. Chem. Phys. Discuss.*, 12, 19209–19241, doi:10.5194/acpd-12-19209-2012, 2012.
- 5 Stoiber, R. E., Williams, S. N., and Huebert, B.: Annual contribution of sulfur dioxide to the atmosphere by volcanoes, *J. Volcanol. Geotherm. Res.*, 33, 1–8, 1987.
- Streets, D. G., Bond, T. M. L., Carmichael, G. R., Fernandes, S., Fu, Q., He, D., Klimont, Z., Nelson, S. M., Tsai, N. Y., Wang, M. Q., Woo, J.-H., and Yarber, K. F.: An inventory of gaseous and primary aerosol emissions in Asia in the year 2000, *J. Geophys. Res.*, 108, 8809, doi:10.1029/2002JD003093, 2003.
- 10 Streets, D. G., Wu, Y., and Chin, M.: Two-decadal aerosol trends as a likely explanation of the global dimming/brightening transition, *Geophys. Res. Lett.*, 33, L15806, doi:10.1029/2006GL026471, 2006.
- Streets, D., Yu, C., Wu, Y., Chin, M., Zhao, Z., Hayasaka, T., and Shi, G.: Aerosol trends over China, 1980–2000, *Aerosol Res.*, 88, 174–182, 2008.
- 15 Streets, D. G., Yan, F., Chin, M., Diehl, T., Mahowald, N., Schultz, M., Wild, M., Wu, Y., and Yu, C.: Anthropogenic and natural contributions to regional trends in aerosol optical depth, 1980–2006, *J. Geophys. Res.*, 114, D00D18, doi:10.1029/2008JD011624, 2009.
- Sutkus, D. J., Baughcum, S. L., and DuBois, D. P.: Scheduled Civil Aircraft Emission Inventories for 1999: Database Development and Analysis, Contractor Report 2001-211216, National Aeronautics and Space Administration, Cleveland, OH, USA, 140 pp., 2001.
- 20 Taylor, K. E., Stouffer, R. J., and Meehl, G. A.: An overview of CMIP5 and the experiment design, *Bull. Amer. Meteor. Soc.*, 93, 485–498, doi:10.1175/BAMS-D-11-00094.1, 2012.
- Textor, C., Schulz, M., Guibert, S., Kinne, S., Balkanski, Y., Bauer, S., Berntsen, T., Berglen, T., Boucher, O., Chin, M., Dentener, F., Diehl, T., Easter, R., Feichter, H., Fillmore, D., Ghan, S., Ginoux, P., Gong, S., Grini, A., Hendricks, J., Horowitz, L., Huang, P., Isaksen, I., Iversen, I., Kloster, S., Koch, D., Kirkevåg, A., Kristjansson, J. E., Krol, M., Lauer, A., Lamarque, J. F., Liu, X., Montanaro, V., Myhre, G., Penner, J., Pitari, G., Reddy, S., Seland, Ø., Stier, P., Takemura, T., and Tie, X.: Analysis and quantification of the diversities of aerosol life cycles within AeroCom, *Atmos. Chem. Phys.*, 6, 1777–1813, doi:10.5194/acp-6-1777-2006, 2006.
- 25 Textor, C., Schulz, M., Guibert, S., Kinne, S., Balkanski, Y., Bauer, S., Berntsen, T., Berglen, T., Boucher, O., Chin, M., Dentener, F., Diehl, T., Feichter, J., Fillmore, D., Ginoux, P., Gong, S., Grini, A., Hendricks, J., Horowitz, L., Huang, P., Isaksen, I. S. A., Iversen, T., Kloster, S., Koch, D., Kirkevåg, A., Kristjansson, J. E., Krol, M., Lauer, A., Lamarque, J. F., Liu, X., Monta-
- 30

**Anthropogenic,
biomass burning, and
volcanic emissions of
BC, OC, and SO₂**

T. Diehl et al.

Title Page

Abstract

Introduction

Conclusions

References

Tables

Figures

◀

▶

◀

▶

Back

Close

Full Screen / Esc

Printer-friendly Version

Interactive Discussion



naro, V., Myhre, G., Penner, J. E., Pitari, G., Reddy, M. S., Seland, Ø., Stier, P., Takemura, T., and Tie, X.: The effect of harmonized emissions on aerosol properties in global models – an AeroCom experiment, *Atmos. Chem. Phys.*, 7, 4489–4501, doi:10.5194/acp-7-4489-2007, 2007.

5 US Standard Atmosphere 1976: US Government Printing Office, Washington, D.C., USA, 1976.

Val Martin, M., Logan, J. A., Kahn, R. A., Leung, F.-Y., Nelson, D. L., and Diner, D. J.: Smoke injection heights from fires in North America: analysis of 5 years of satellite observations, *Atmos. Chem. Phys.*, 10, 1491–1510, doi:10.5194/acp-10-1491-2010, 2010.

10 van der Werf, G. R., Randerson, J. T., Giglio, L., Collatz, G. J., Kasibhatla, P. S., and Arelano Jr., A. F.: Interannual variability in global biomass burning emissions from 1997 to 2004, *Atmos. Chem. Phys.*, 6, 3423–3441, doi:10.5194/acp-6-3423-2006, 2006.

van der Werf, G. R., Randerson, J. T., Giglio, L., Collatz, G. J., Mu, M., Kasibhatla, P. S., Morton, D. C., DeFries, R. S., Jin, Y., and van Leeuwen, T. T.: Global fire emissions and the contribution of deforestation, savanna, forest, agricultural, and peat fires (1997–2009), *Atmos. Chem. Phys.*, 10, 11707–11735, doi:10.5194/acp-10-11707-2010, 2010.

15 Vestreng, V., Myhre, G., Fagerli, H., Reis, S., and Tarrasón, L.: Twenty-five years of continuous sulphur dioxide emission reduction in Europe, *Atmos. Chem. Phys.*, 7, 3663–3681, doi:10.5194/acp-7-3663-2007, 2007.

Westphal, L. and Toon, O. B.: Simulations of Microphysical, Radiative, and Dynamical Processes in a Continental-Scale Forest Fire Smoke Plume, *J. Geophys. Res.*, 96, 22379–22400, doi:10.1029/91JD01956, 1991.

20 Wooster, M. J., Roberts, G., Perry, G. L. W., and Kaufman, Y. J.: Retrieval of biomass combustion rates and totals from fire radiative power observations: FRP derivation and calibration relationships between biomass consumption and fire radiative energy release, *J. Geophys. Res.*, 110, D24311, doi:10.1029/2005JD006318, 2005.

25 Yoon, J., von Hoyningen-Huene, W., Vountas, M., and Burrows, J. P.: Analysis of linear long-term trend of aerosol optical thickness derived from SeaWiFS using BAER over Europe and South China, *Atmos. Chem. Phys.*, 11, 12149–12167, doi:10.5194/acp-11-12149-2011, 2011.

Anthropogenic, biomass burning, and volcanic emissions of BC, OC, and SO₂

T. Diehl et al.

[Title Page](#)

[Abstract](#) [Introduction](#)

[Conclusions](#) [References](#)

[Tables](#) [Figures](#)

[⏪](#) [⏩](#)

[◀](#) [▶](#)

[Back](#) [Close](#)

[Full Screen / Esc](#)

[Printer-friendly Version](#)

[Interactive Discussion](#)

Table 1. Range (minimum to maximum) of emissions during the period 1980 to 2005 and emissions for the year 2005. Units are Tg(species) yr⁻¹. “GLB”=Global land-based, “MAPv2”=A2-MAP-v2 and “ACCMIP”=A2-ACCMIP. We evaluated regional biomass burning emissions only for OC. Volcanic emissions from A2-MAP are included in the “Total 2005” emissions for A2-ACCMIP.

| | | BC | | OC | | SO ₂ | |
|--------------------|-------|---------------|---------------|---------------|-----------|-----------------|-----------|
| | | MAPv2 | ACCMIP | MAPv2 | ACCMIP | MAPv2 | ACCMIP |
| USA | Range | 0.29–0.52 | 0.28–0.41 | 0.44–0.68 | 0.42–0.70 | 10.5–26.9 | 10.3–19.7 |
| | 2005 | 0.33 | 0.28 | 0.47 | 0.42 | 10.5 | 10.3 |
| OECD | Range | 0.26–0.37 | 0.30–0.35 | 0.25–0.36 | 0.31–0.43 | 5.86–22.5 | 3.98–22.0 |
| | 2005 | 0.30 | 0.30 | 0.26 | 0.31 | 5.86 | 3.98 |
| Europe | Range | 0.12–0.28 | 0.11–0.19 | 0.24–0.51 | 0.31–0.46 | 3.01–10.4 | 4.50–12.3 |
| | 2005 | 0.13 | 0.11 | 0.25 | 0.35 | 3.01 | 4.50 |
| Former USSR | Range | 0.15–0.75 | 0.23–0.85 | 0.18–0.81 | 0.99–1.83 | 10.7–30.4 | 6.45–16.7 |
| | 2005 | 0.15 | 0.23 | 0.18 | 0.99 | 10.8 | 6.45 |
| South Asia | Range | 0.35–0.65 | 0.37–0.68 | 1.09–1.69 | 1.30–2.14 | 2.31–7.50 | 1.66–6.84 |
| | 2005 | 0.65 | 0.68 | 1.69 | 2.14 | 7.50 | 6.84 |
| East Asia | Range | 1.09–1.74 | 0.97–1.61 | 1.63–2.27 | 2.28–3.05 | 14.7–35.9 | 11.8–26.1 |
| | 2005 | 1.74 | 1.61 | 2.24 | 3.01 | 35.9 | 26.1 |
| GLB antrop. | Range | 4.58–5.31 | 4.50–5.18 | 7.71–8.91 | 11.0–12.8 | 104–143 | 92.6–120 |
| | 2005 | 5.31 | 5.18 | 8.91 | 12.8 | 113.4 | 96.7 |
| Ship | Range | 0.04–0.06 | 0.08–0.14 | 0.10–0.15 | 0.09–0.15 | 4.20–7.84 | 6.94–13.0 |
| | 2005 | 0.06 | 0.14 | 0.15 | 0.15 | 7.84 | 13.0 |
| Aircraft | Range | 0.0052–0.0092 | 0.0034–0.0056 | 0.0017–0.0031 | – | 0.086–0.140 | – |
| | 2005 | 0.0092 | 0.0056 | 0.0031 | – | 0.140 | – |
| | | BC | | OC | | SO ₂ | |
| | | MAPv2 | ACCMIP | MAPv2 | ACCMIP | MAPv2 | ACCMIP |
| NAB | Range | – | – | 0.10–1.53 | 0.11–1.60 | – | – |
| | 2005 | – | – | 0.61 | 0.50 | – | – |
| EAB | Range | – | – | 1.09–7.64 | 0.14–7.03 | – | – |
| | 2005 | – | – | 1.35 | 1.12 | – | – |
| SAM | Range | – | – | 2.64–8.05 | 1.49–4.82 | – | – |
| | 2005 | – | – | 8.05 | 4.82 | – | – |
| NAF | Range | – | – | 8.85–12.4 | 3.58–6.36 | – | – |
| | 2005 | – | – | 10.21 | 4.37 | – | – |
| SAF | Range | – | – | 8.15–12.6 | 3.37–6.00 | – | – |
| | 2005 | – | – | 10.75 | 4.46 | – | – |
| SEA | Range | – | – | 2.76–20.9 | 1.34–13.7 | – | – |
| | 2005 | – | – | 5.77 | 3.66 | – | – |
| Global BB | Range | 4.52–7.05 | 1.79–3.52 | 36.2–56.4 | 14.4–33.1 | 5.42–8.46 | 2.04–6.61 |
| | 2005 | 5.25 | 2.57 | 42.02 | 21.88 | 6.30 | 3.61 |
| Volcanic emissions | Range | – | – | – | – | 22.1–51.7 | – |
| | 2005 | – | – | – | – | 26.7 | (26.7) |
| Total | 2005 | 10.63 | 7.90 | 51.08 | 34.83 | 154.38 | 140.01 |



**Anthropogenic,
biomass burning, and
volcanic emissions of
BC, OC, and SO₂**

T. Diehl et al.

[Title Page](#)[Abstract](#)[Introduction](#)[Conclusions](#)[References](#)[Tables](#)[Figures](#)[I◀](#)[▶I](#)[◀](#)[▶](#)[Back](#)[Close](#)[Full Screen / Esc](#)[Printer-friendly Version](#)[Interactive Discussion](#)**Table 2.** Globally averaged emission index of black carbon as a function of altitude (from Döpelheuer, 2002).

| Altitude (km) | Emission index (g(BC) kg(fuel) ⁻¹) |
|------------------|---|
| 0.0 | 0.08 |
| 0.5 | 0.1 |
| 1.5 | 0.09 |
| 2.5 | 0.08 |
| 3.5 | 0.07 |
| 4.5 | 0.06 |
| 5.5 | 0.06 |
| 6.5 | 0.04 |
| 7.5 | 0.04 |
| 8.5 | 0.04 |
| 9.5 | 0.03 |
| 10.5 | 0.03 |
| 11.5 | 0.02 |
| 12.5 | 0.05 |
| 13.5 | 0.07 |
| 14.5 | 0.07 |
| 15.5 | 0.07 |
| 16.5 | 0.08 |

Anthropogenic, biomass burning, and volcanic emissions of BC, OC, and SO₂

T. Diehl et al.

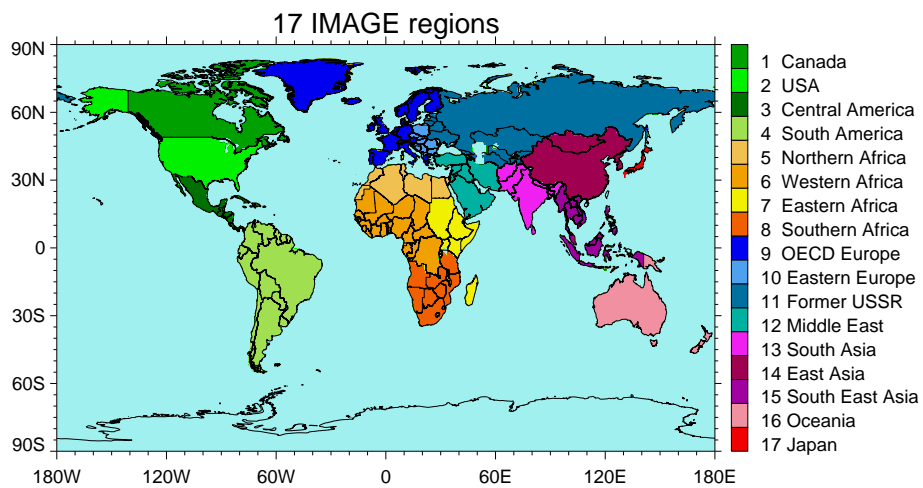


Fig. 1. 17 regions from the IMAGE model as used for the A2-MAP land-based anthropogenic emissions.

Title Page

Abstract

Introduction

Conclusions

References

Tables

Figures

⏪

⏩

◀

▶

Back

Close

Full Screen / Esc

Printer-friendly Version

Interactive Discussion



Anthropogenic (land-based) SO₂ Emission

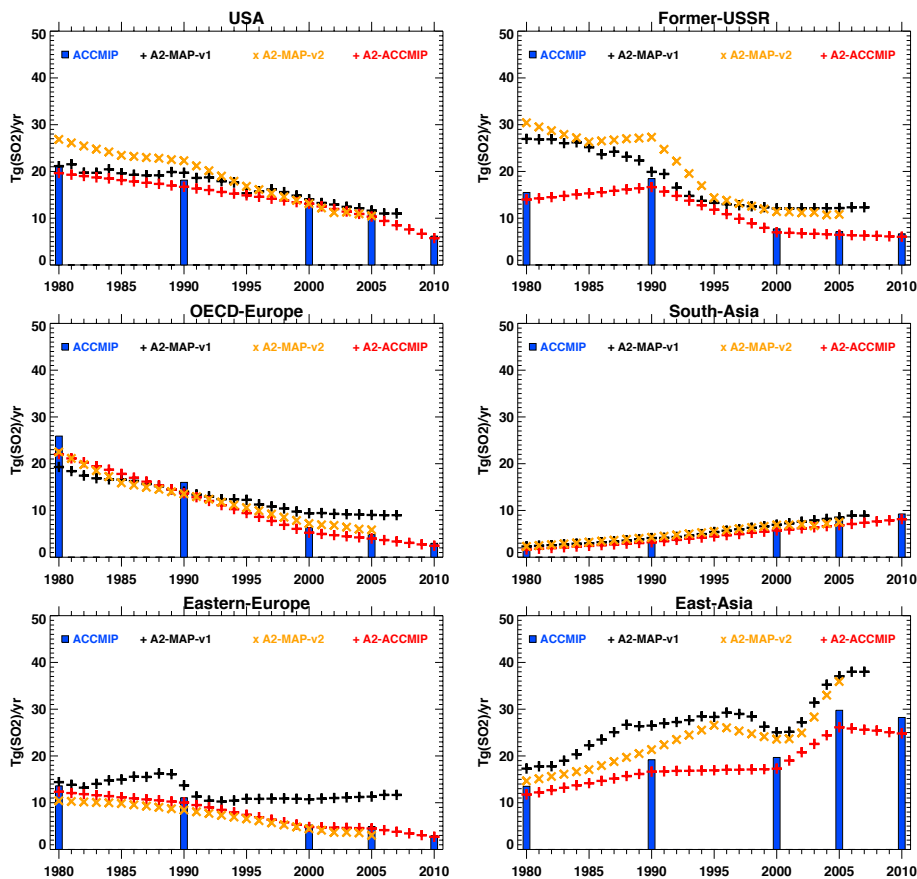


Fig. 2. Regional trends of land-based SO₂ emissions in Tg yr⁻¹ for 6 regions.

24942

ACPD

12, 24895–24954, 2012

**Anthropogenic,
biomass burning, and
volcanic emissions of
BC, OC, and SO₂**

T. Diehl et al.

Title Page

Abstract

Introduction

Conclusions

References

Tables

Figures

◀

▶

◀

▶

Back

Close

Full Screen / Esc

Printer-friendly Version

Interactive Discussion



Anthropogenic (land-based) BC Emission

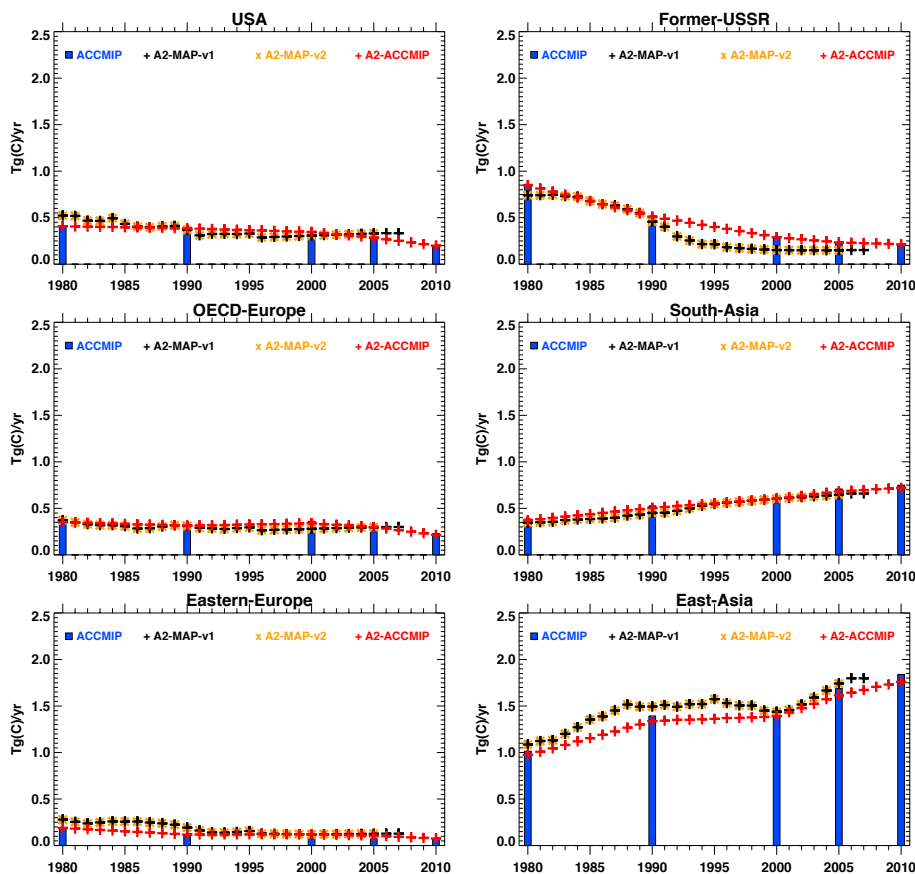


Fig. 3. Regional trends of land-based BC emissions in Tgyr⁻¹ for 6 regions.

Anthropogenic (land-based) OC Emission

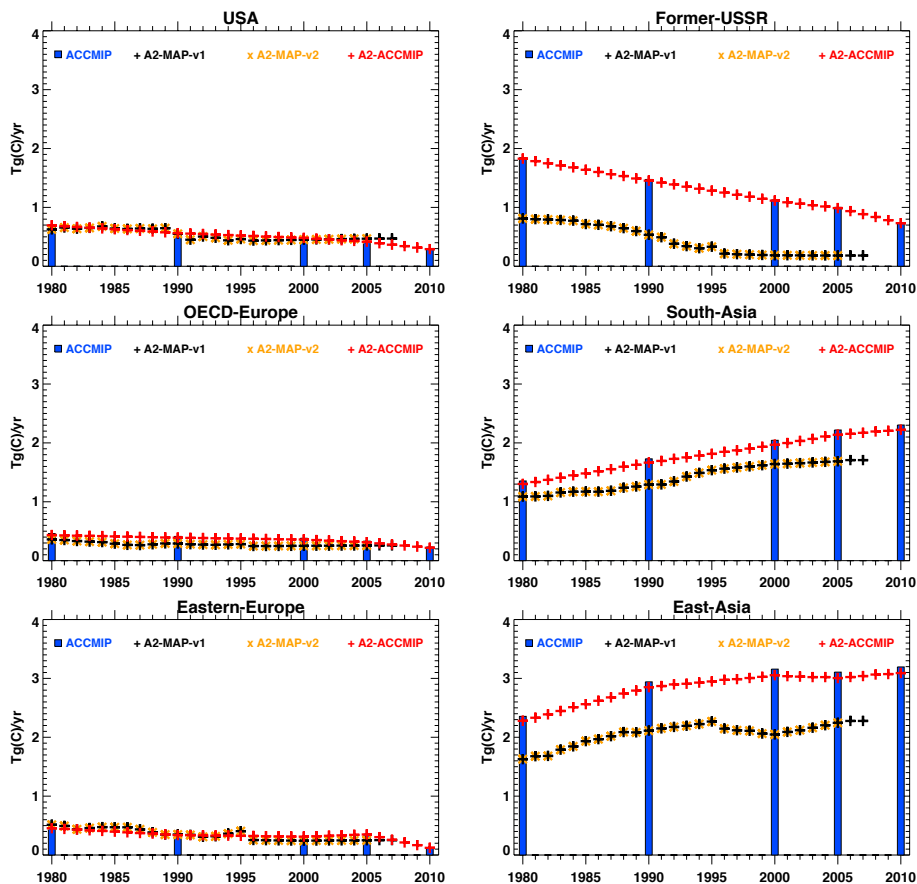


Fig. 4. Regional trends of land-based OC emissions in Tg(C)^{-1} for 6 regions.

24944

Title Page

Abstract

Introduction

Conclusions

References

Tables

Figures

⏪

⏩

◀

▶

Back

Close

Full Screen / Esc

Printer-friendly Version

Interactive Discussion



Anthropogenic, biomass burning, and volcanic emissions of BC, OC, and SO₂

T. Diehl et al.

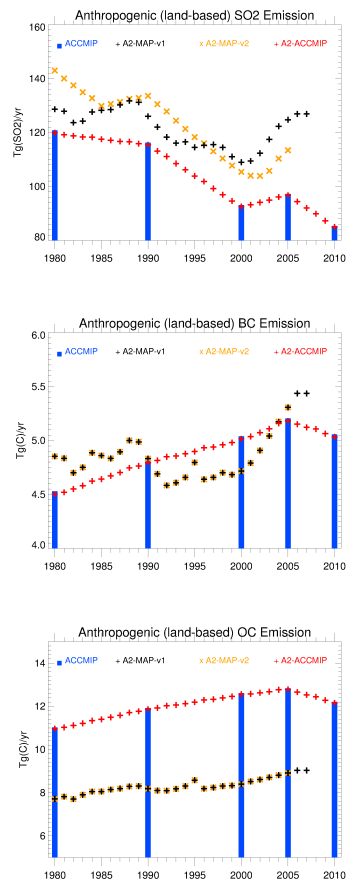


Fig. 5. Trends of global land-based SO₂, BC, and OC emissions in Tg yr⁻¹.

[Title Page](#)

[Abstract](#) | [Introduction](#)

[Conclusions](#) | [References](#)

[Tables](#) | [Figures](#)

[⏪](#) | [⏩](#)

[◀](#) | [▶](#)

[Back](#) | [Close](#)

[Full Screen / Esc](#)

[Printer-friendly Version](#)

[Interactive Discussion](#)



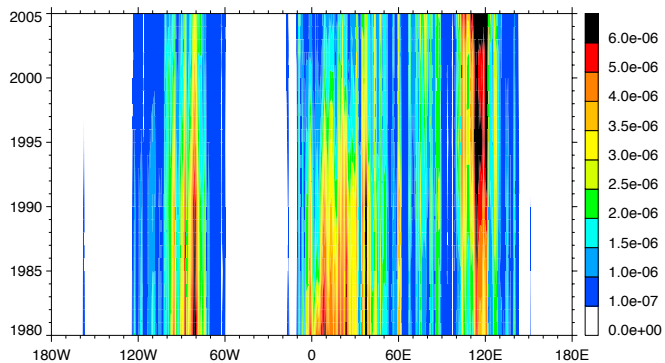
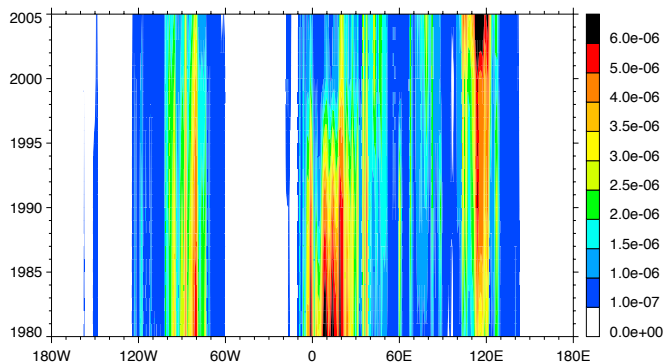


Fig. 6. Hovmoeller diagrams of land-based anthropogenic SO₂ emissions in the Northern Hemisphere for A2-ACCMIP (top) and A2-MAP-v2 (bottom). These are annual values and the unit is kg m⁻² d⁻¹.

Anthropogenic, biomass burning, and volcanic emissions of BC, OC, and SO₂

T. Diehl et al.

Title Page

Abstract Introduction

Conclusions References

Tables Figures

⏪ ⏩

◀ ▶

Back Close

Full Screen / Esc

Printer-friendly Version

Interactive Discussion



Anthropogenic, biomass burning, and volcanic emissions of BC, OC, and SO₂

T. Diehl et al.

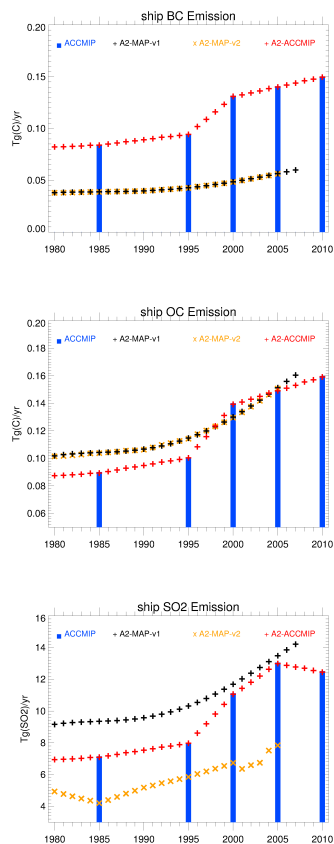


Fig. 7. Trends of global emissions from ocean-going vessels for BC, OC, and SO₂ in Tgyr⁻¹. ACCMIP ship emissions labeled “1980” and “1990” are actually snapshots of the years 1985 and 1995, respectively. We therefore placed the ACCMIP bars next to 1985 and 1995.

Title Page

Abstract Introduction

Conclusions References

Tables Figures

⏪ ⏩

◀ ▶

Back Close

Full Screen / Esc

Printer-friendly Version

Interactive Discussion



Anthropogenic, biomass burning, and volcanic emissions of BC, OC, and SO₂

T. Diehl et al.

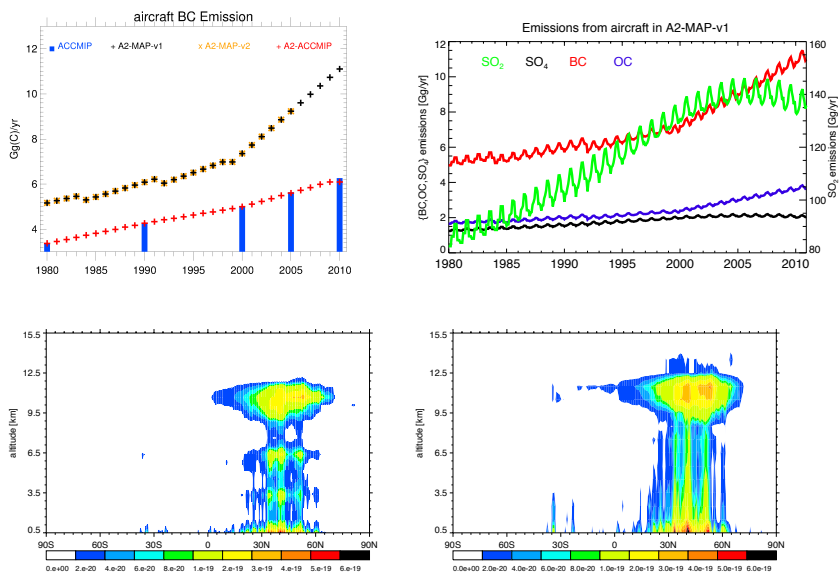


Fig. 8. Global aircraft emissions of annual BC for A2-MAP and A2-ACCMIP in Ggyr^{-1} (top left), SO_2 , SO_4 , BC, and OC with seasonal variation for A2-MAP in Ggyr^{-1} (top right), zonally averaged BC for 1999 and A2-ACCMIP in $\text{kgm}^{-3}\text{s}^{-1}$ (bottom left), and zonally averaged BC for 1999 and A2-MAP in $\text{kgm}^{-3}\text{s}^{-1}$ (bottom right).

[Title Page](#)
[Abstract](#)
[Introduction](#)
[Conclusions](#)
[References](#)
[Tables](#)
[Figures](#)
[⏪](#)
[⏩](#)
[◀](#)
[▶](#)
[Back](#)
[Close](#)
[Full Screen / Esc](#)
[Printer-friendly Version](#)
[Interactive Discussion](#)

**Anthropogenic,
biomass burning, and
volcanic emissions of
BC, OC, and SO₂**

T. Diehl et al.

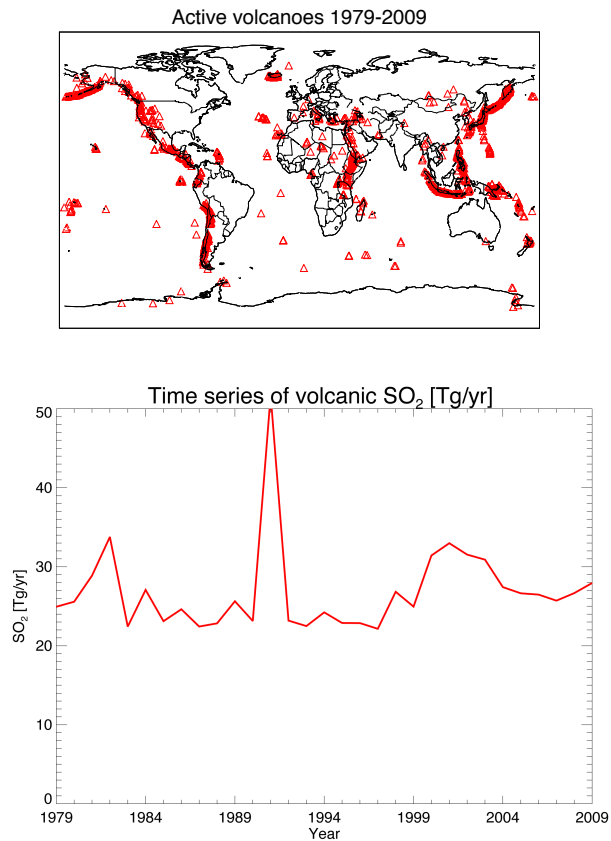


Fig. 9. Locations of active volcanoes and time series of global volcanic SO₂ emissions in Tgyr⁻¹.

[Title Page](#)[Abstract](#)[Introduction](#)[Conclusions](#)[References](#)[Tables](#)[Figures](#)[◀](#)[▶](#)[◀](#)[▶](#)[Back](#)[Close](#)[Full Screen / Esc](#)[Printer-friendly Version](#)[Interactive Discussion](#)

Anthropogenic, biomass burning, and volcanic emissions of BC, OC, and SO₂

T. Diehl et al.

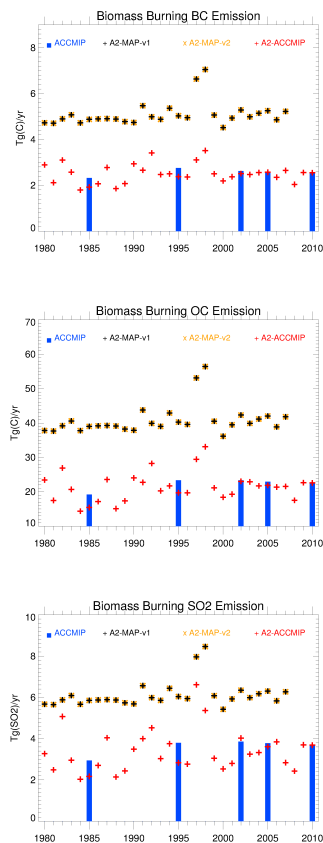


Fig. 10. Global biomass burning emissions for BC, OC, and SO₂ in Tgyr⁻¹.

[Title Page](#)

[Abstract](#) | [Introduction](#)

[Conclusions](#) | [References](#)

[Tables](#) | [Figures](#)

[⏪](#) | [⏩](#)

[◀](#) | [▶](#)

[Back](#) | [Close](#)

[Full Screen / Esc](#)

[Printer-friendly Version](#)

[Interactive Discussion](#)



**Anthropogenic,
biomass burning, and
volcanic emissions of
BC, OC, and SO₂**

T. Diehl et al.

Title Page

Abstract

Introduction

Conclusions

References

Tables

Figures

◀

▶

◀

▶

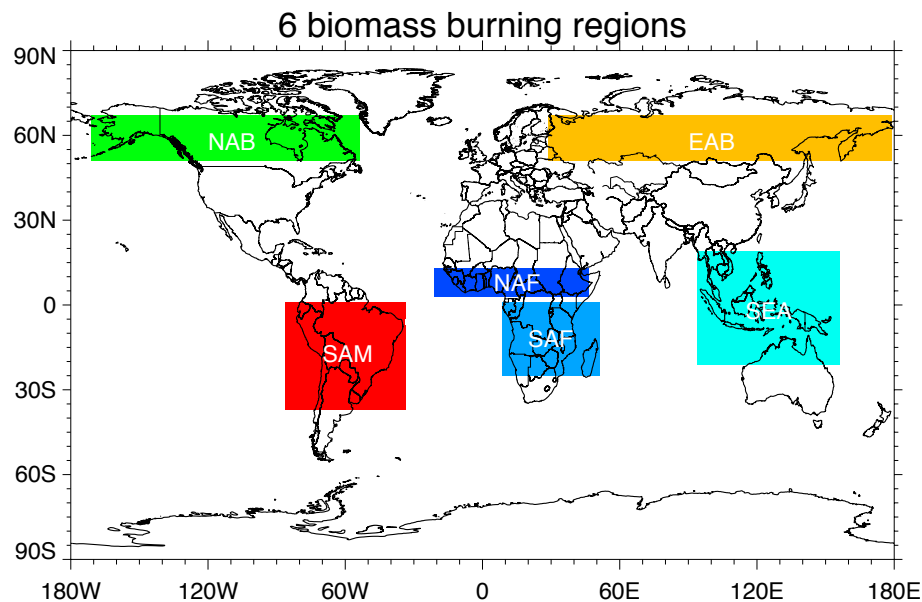
Back

Close

Full Screen / Esc

Printer-friendly Version

Interactive Discussion

**Fig. 11.** Definition of 6 biomass burning regions used for regional analysis of OC emissions.

Biomass Burning OC Emission

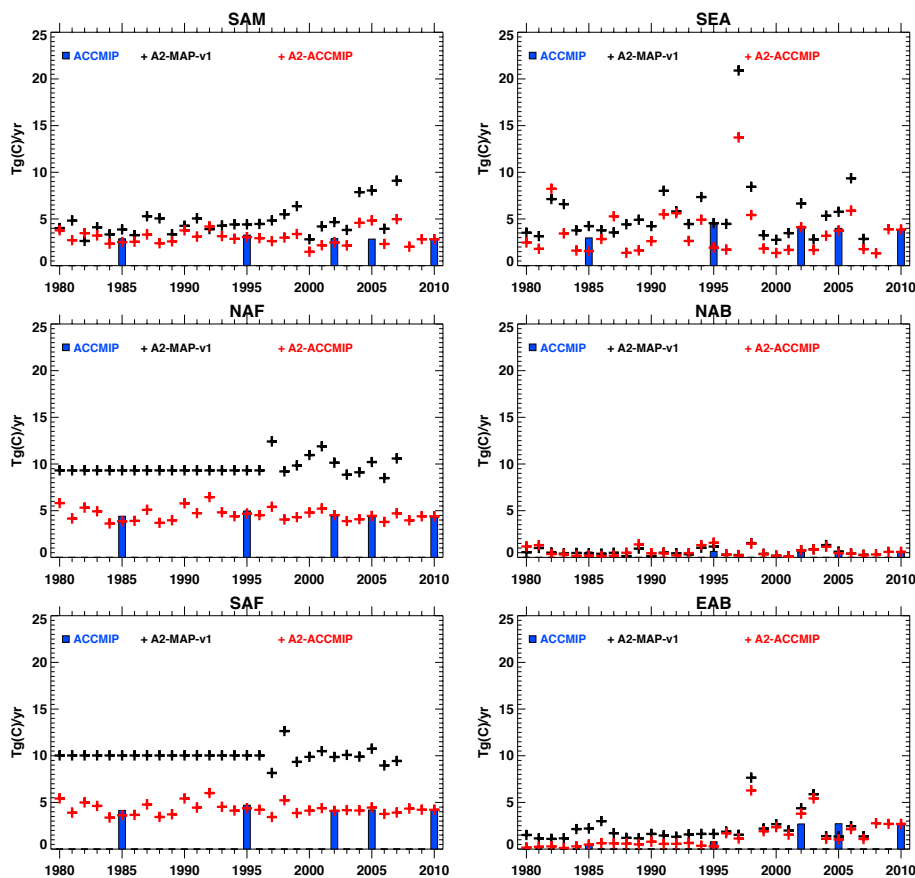


Fig. 12. Regional biomass burning OC emissions for 6 regions in Tgyr^{-1} .

24952

ACPD

12, 24895–24954, 2012

**Anthropogenic,
biomass burning, and
volcanic emissions of
BC, OC, and SO_2**

T. Diehl et al.

Title Page

Abstract

Introduction

Conclusions

References

Tables

Figures

⏪

⏩

◀

▶

Back

Close

Full Screen / Esc

Printer-friendly Version

Interactive Discussion



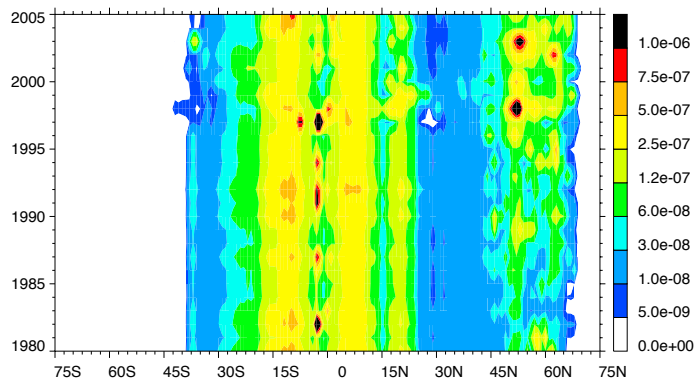
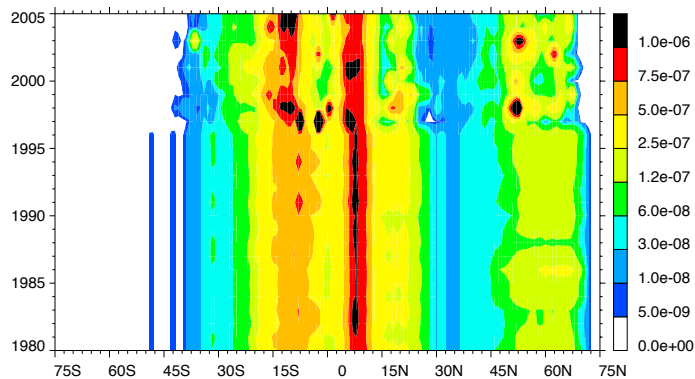


Fig. 13. Hovmoeller diagrams of OC biomass burning emissions for A2-MAP (top) and A2-ACCMIP (bottom). These are yearly averaged values and the unit is $\text{kg m}^{-2} \text{d}^{-1}$.

Anthropogenic, biomass burning, and volcanic emissions of BC, OC, and SO₂

T. Diehl et al.

Title Page

Abstract Introduction

Conclusions References

Tables Figures

◀ ▶

◀ ▶

Back Close

Full Screen / Esc

Printer-friendly Version

Interactive Discussion



Biomass Burning OC Emission

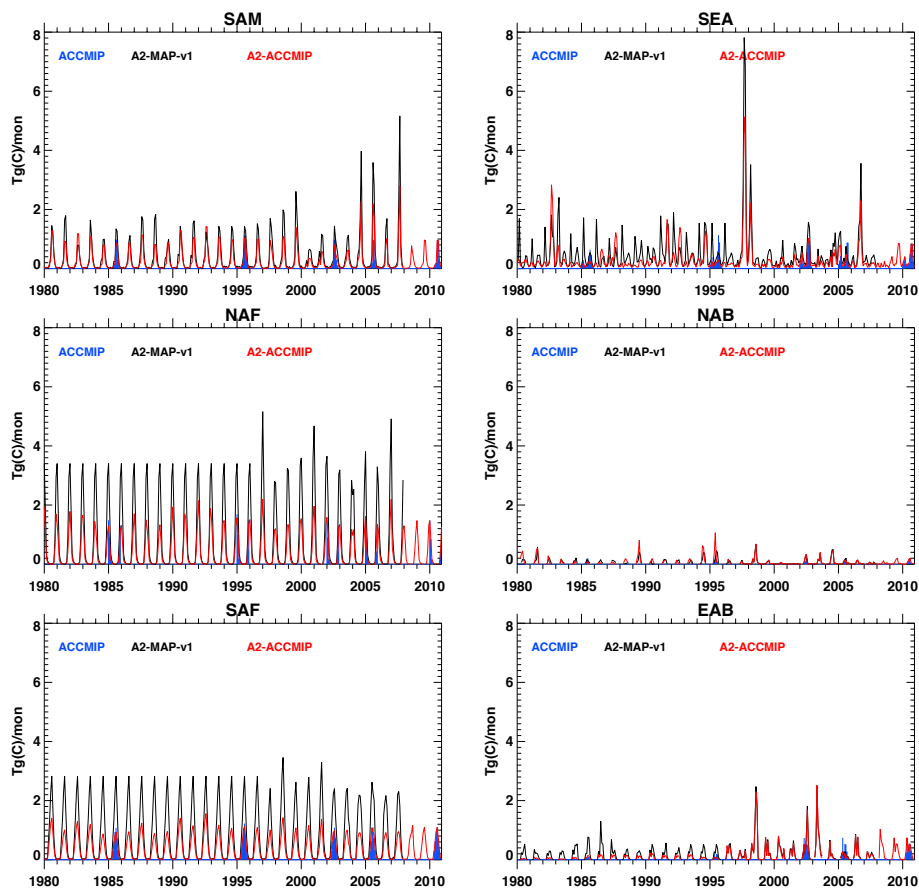


Fig. 14. Seasonal variation of biomass burning OC emissions for 6 regions in Tg month⁻¹.